Molecular applications of analytical gradient approach for the improved virtual orbital-complete active space configuration interaction method

Rajat K. Chaudhuri,[1,a)] Sudip Chattopadhyay,[2,b)] Uttam Sinha Mahapatra,[3,c)] and Karl F. Freed[4,d)]
[1]*Indian Institute of Astrophysics, Bangalore 560034, India*
[2]*Department of Chemistry, Bengal Engineering and Science University, Shibpur, Howrah 711103, India*
[3]*Department of Physics, Taki Government College, Taki, North 24 Parganas, India*
[4]*Department of Chemistry, The James Franck Institute, University of Chicago, Chicago, Illinois 60637, USA*

(Received 11 September 2009; accepted 16 December 2009; published online 20 January 2010)

The improved virtual orbital-complete active space configuration interaction (IVO-CASCI) method is extended to determine the geometry and vibrational frequencies for ground and *excited* electronic states using an analytical total energy gradient scheme involving both first and second order analytical derivatives. Illustrative applications consider the ground state geometries of the benzene (C_6H_6), biphenyl ($C_{12}H_{10}$), and alanine dipeptide ($CH_3CONHCHCH_3CONHCH_3$) molecules. In addition, the IVO-CASCI geometry optimization has been performed for the first excited singlet ($^1B_{2u}$) and triplet states ($^3B_{1u}$) of benzene to assess its applicability for excited and open-shell systems. The D_{6h} symmetry benzene triplet optimization produces a saddle point, and a descent along the unstable mode produces the stable minimum. Comparisons with Hartree–Fock, second order Möller–Plesset perturbation theory, complete active space self-consistent field (CASSCF), and density functional theory demonstrate that the IVO-CASCI approach generally fares comparable to or better for all systems studied. The vibrational frequencies of the benzene and biphenyl molecules computed with the analytical gradient based IVO-CASCI method agree with the experiment and with other accurate theoretical estimates. Satisfactory agreement between our results, other benchmark calculations, and available experiment demonstrates the efficacy and potential of the method. The close similarity between CASSCF and IVO-CASCI optimized geometries and the greater computational efficiency of the IVO-CASCI method suggests the replacement of CASSCF treatments by the IVO-CASCI approach, which is free from the convergence problems that often plague CASSCF treatments. © *2010 American Institute of Physics*. [doi:10.1063/1.3290203]

I. INTRODUCTION

Since gradient approaches are extremely useful tools in quantum chemistry, considerable effort has been devoted to the development of analytic derivative approaches for an increasing array of *ab initio* methods.[1,2] Gradient methods facilitate the routine study of equilibrium geometries, transition states, intrinsic reaction coordinates (IRCs), vibrational frequencies, energy relaxation processes, and dynamics of molecular systems by determining the derivatives of the adiabatic potential energy surface(s) (for both ground and excited states) of a molecule with respect to the nuclear coordinate(s). Analytic derivatives also provide important applications to the calculations of various electrical and magnetic properties where the derivatives are taken with respect to the external field.

The seminal work of Pulay in developing a practical method for evaluating analytical gradients[3] of the SCF energy has opened fresh avenues for the study of molecular force fields.[4] Subsequent extensions by Pople *et al.*[5] of this approach treat contributions to the correlation energy by implementing analytical gradients for the second order many-body perturbation theory (MBPT) method. Genuinely important breakthroughs in the early 1980s enabled simplified gradient calculations for correlated many-body methods, including the state-of-the-art Z-vector technique of Handy and Schaefer[2] for eliminating the terms involving derivatives of the molecular orbital (MO) coefficients in MBPT and coupled cluster (CC) methods.[6] These developments essentially provide the foundation for tremendous progress, culminating in the genesis of theoretical methods for evaluating the gradients, for example, of the MBPT energy all the way through fourth order.[7–12] The study of analytic derivatives for CC methods[13] has recently culminated in analytic gradient theories for equations of motion CC[14] and propagator approaches[15] that are appropriate for specialized studies of excited electronic states and certain open-shell systems.

Single reference (SR) approaches provide a standard tool for highly accurate computations of small to medium sized molecules near the equilibrium region of closed shell ground

[a)]Electronic mail: rkchaudh@iiap.res.in.
[b)]Electronic mail: sudip_chattopadhyay@rediffmail.com.
[c)]Electronic mail: uttam.mahapatra@linuxmail.org.
[d)]Electronic mail: freed@uchicago.edu.

electronic states. However, SR methods (truncated at low orders) have difficulties in treating quasidegenerate situations, such as bond breaking, transition states, and so on. When a near degeneracy is present, the wave functions become essentially multiconfigurational in nature, and both dynamical and nondynamical correlation contributions are essential to obtain accurate and stable descriptions of the energy and its derivatives. Consequently, multireference approaches represent the natural point of departure for treating quasidegenerate systems.[16]

Several attempts have been made to formulate efficient multireference methods[17–19] that bypass the inherent difficulties associated with SR treatments because the derivatives of a molecular potential energy surface with pronounced multireference character (as in excited or transition states) are more appropriately treated with genuine multireference approaches. However, the formal implementation of analytic gradient approaches for general multireference many-body methods is nontrivial and to our knowledge, only a few studies consider numerical calculations for the gradient of multireference wave functions.[20–24]

Among multireference approaches, the complete active space self-consistent field (CASSCF) scheme is one of the most widely used methods for determining the ground and excited state geometries and vibrational frequencies. This method is popular partly because it is (a) stable over the entire potential surface when an appropriate active space is considered and (b) available in almost all quantum chemistry packages, including *open-source programs*. While the CASSCF method is capable of providing reliable predictions of the ground and excited state geometries and vibrational frequencies, the procedure rapidly becomes prohibitive since the dimension of the CAS grows very rapidly with an increasing number of active electron and orbitals. Moreover, because the CASSCF method is iterative in nature, computations with larger active spaces often become plagued with convergence difficulties. The convergence problems can partly be mitigated by using a smaller active space, but then the quality of the zeroth order wave functions may degrade.

To alleviate the problem associated with the CASSCF step, a number of groups[25–30] have proposed the possibility of avoiding the CASSCF step by using orbitals obtained from simpler methods to construct the active spaces for use in subsequent multireference perturbative and nonperturbative treatments. In this connection, Freed and co-workers[25–28] demonstrated that the convergence problems of the CASSCF procedure can be circumvented efficiently by using the computationally inexpensive "improved virtual orbital-complete active space configuration interaction" (IVO-CASCI) technique. The IVO-CASCI approach has the benefits that (i) it does not require iterations beyond those in the initial SCF calculation, (ii) the variational character of the IVO-CASCI scheme suggests that the derivatives can be easily obtained via the Hellmann–Feynman theorem, (iii) it can handle multireference systems in a balanced manner, (iv) it maintains size consistency, (v) the IVO-CASCI method provides a much more accurate description of excited state than the configuration interaction singles (CIS) method, (vi) the energy is invariant to rotations of orbitals within the same CAS space, and finally (vii) it does not require full four-index transformation of atomic orbital (AO) to MO integrals. These features provide a unique niche for the IVO-CASCI method that enables us to treat much larger molecules using the full "chemical" valence space, which, often, is not possible for CASSCF calculations. Previous IVO-CASCI computations for atomic spectra,[31,32] global potential energy surfaces,[26,27] and electronic spectra of complex molecular systems[25,28] clearly indicate the efficacy of the method. Thus, computational costs of high level methods for the simultaneous inclusion of static and dynamic correlation effects [such as MRMP2,[33] multiconfigurational quasidegenerate perturbation theory (MCQDPT),[34] CASPT2,[35] and so on] would be considerably improved by combining them with the IVO-CASCI scheme.

Recent calculations by Chaudhuri *et al.*[36] combine the IVO-CASCI approach with multireference Möller–Plesset perturbation theory[33] and MCQDPT (Ref. 34) methods to append dynamical correlation into the IVO-CASCI energy and wave function. These recent studies[36–39] further demonstrate that the improved virtual orbital multireference Möller–Plesset (IVO-MRMP)/MCQDPT approaches offer very promising tools for investigating geometries and potential energy surfaces for electronic states that are strongly perturbed by intruders and/or that have pronounced multireference character. Another approach for skipping the expensive orbital optimization step is the multireference Möller–Plesset complete active space configuration interaction method of Hirao and co-workers[29] that involves optimization of only the expansion coefficients of the full configuration interaction (CI) configurations in an active space.

Recently, Chaudhuri and Freed[40] applied the IVO-CASCI procedure to determine the equilibrium geometries and vibrational frequencies of di- and triatomic molecules using *numerically* determined energy gradients. Their study clearly demonstrates that the geometries and vibrational frequencies from IVO-CASCI calculations are generally comparable to or better than those provided by CASSCF treatments with the same size of CAS (and other computationally inexpensive methods) and that the converged IVO-CASCI geometries are often obtained with smaller CASs than that required by the CASSCF scheme.[40] Given the successes of the IVO-CASCI numerical gradients, we have developed the corresponding far more efficient analytic derivative version that is used here to compute the optimized structural parameters and associated properties using both first and second order *analytical energy gradients*. This approach is computationally efficient and robust from the standpoint of numerical stability. Moreover, it is free from root flipping, intruder states, size-consistency errors, and other problems associated with most multireference methods. Our illustrative applications consider the benzene (C_6H_6), biphenyl ($C_{12}H_{10}$), and alanine dipeptide ($C_6H_{12}O_2N_2$) molecules. These are excellent examples to illustrate the potentiality and reliability of any electronic structure theory due to multiple interacting electronic states (an indication for the importance of nondynamical correlation), which complicate the description of their ground and excited states. Thus, the ground/excited state geometries of these systems are computed using the

IVO-CASSCI method with *analytically* determined energy gradients. The computed geometries and vibrational frequencies (for benzene and biphenyl) are compared with experiment and with those obtained using the same basis set and the Hartree–Fock (HF), MP2, and Becke-3-Lee–Yang–Parr (B3LYP) (Ref. 41) density functional theories. The systems considered are not only complex but are also of fundamental spectroscopic interest. For example, the $S_0(X\ ^1A_g) \rightarrow S_1(1\ ^1B_{2u})$ transition of benzene is considered as a benchmark study in computational chemistry because the vibrational structure of this transition is well documented and because it is a prototypical system for studying radiationless transitions.[42] The benzene triplet state provides an example in which symmetry breaking occurs. While the ground state conformers of alanine dipeptide are not multireference, the system is central to the development of force fields for proteins.

The numerical implementation for various nontrivial systems demonstrates that the equilibrium geometries and vibrational frequencies are well reproduced by the analytic gradient based IVO-CASCI approach, and, consequently, the IVO-CASCI approach represents a nice compromise between the computational efficiency and accuracy with respect to the CASSCF method, which has been well established as the method of choice for multireference mean-field computations of small-to-medium sized molecules.

II. THEORY

In this section, we briefly review only those necessary details for the evaluation of the analytic energy gradient with respect to nuclear displacements for CASCI/multiconfiguration self-consistent field (MCSCF) wave functions because the remaining details may be extracted from the available literature.[43,44]

The analytic energy gradient of a CI wave function decomposes into two types of terms. The skeleton terms reflect the changes in the AOs, and these contributions have the same form as the full energy expression, except that derivative integrals replace the regular integrals. The remaining terms reflect changes in the MOs and involve the orbital response coefficients, which are determined by solving the first order coupled-perturbed Hartree–Fock (CPHF) or coupled-perturbed multiconfiguration Hartree–Fock (CPMCHF) equations, depending upon the reference function employed in constructing the configuration state function(s) (CSF). The essential difference between the CPHF and CPMCHF equations is that the derivatives of MO coefficients are the only unknowns in the CPHF equations, whereas the derivatives of the MOs and of the CI coefficients are the unknowns in CPMCHF equations.

As noted by Yamaguchi *et al.*,[44] the explicit evaluation of the first derivatives of the MO and CI coefficients is *not necessary* for the determination of the first derivative of the MCSCF energy. This simplification also applies for closed-shell or restricted open-shell HF functions. However, the evaluation of the second derivative of the HF/MCSCF energy requires knowledge of the first order variations in the MO and CI coefficients (but not for the HF wave function) with respect to nuclear displacements. In contrast, the derivatives of the CI coefficients generally require the computation of MO derivatives because the MOs are not variationally optimized in the CI procedure. At this juncture, we emphasize that the IVOs are variationally optimized, although they are determined by a unitary transformation instead of an iterative procedure.

The following (Sec. II A) provides a minimal basic description, which suffices to introduce the IVO-CASCI method for the general reader. The methods for the evaluation of the analytic energy gradient for a CASCI/MCSCF wave functions are described in Sec. II B.

A. Generation of improved virtual orbitals

One portion of both the IVO-CASCI and CASSCF procedures effectively involves a CASCI computation, where the CAS comprises all configurations with filled core, empty excited orbitals, and the remaining electrons distributed among the active valence orbitals in all possible ways. The CASSCF orbitals are optimized for a single state or for some weighted average of several states, while the IVO-CASCI orbitals do not require optimization to achieve at least a comparable accuracy. The reasons for this counterintuitive behavior are as follows: a CI computation of dimension D is well known to provide rigorous upper bounds to the energies of the D lowest electronic states,[45] but, of course, accurate bounds are expected only for the lowest few of these states, which fortunately, are generally the states of interest. However, the use of orbitals optimized for one (or for the average of a few) states generally yields a poor representation of the other states, and this feature is partially responsible for the poor convergence of the CASSCF procedure as the dimension of the CAS grows. Our alternative approach involves directly choosing orbitals that simultaneously provide a good representation for several of the lowest lying electronic states. This procedure has previously been followed in H^v (Ref. 16) computations where the CAS orbitals are defined as comprising the highest occupied orbitals (perhaps, only for certain symmetries) in the SCF approximation to the ground (or a low lying) state and a set of the lowest lying IVO orbitals constructed from the remaining unoccupied space in the basis set. This IVO approach is designed to maximize the accuracy of the first order H^v approximation, which is equivalent to a CASCI, for the low lying electronic states in order to minimize the required perturbative corrections.[27] Earlier H^v computations use a computationally complex sequence of SCF computations to obtain the IVOs, but more recently they employ a simple direct method for generating the IVOs for several common situations.[25] The significant improvement in computational efficiency for determining the IVOs is one important feature contributing to the packageability of the IVO-CASCI method and its use for geometry optimization.

Since the basic philosophy of generating the IVOs is the same for both restricted and unrestricted HF orbitals, we only present the restricted HF case, which is used herein. When the ground state of the system is a closed shell, we begin with the HF MOs for the ground state wave-function

$\Phi_0 = \mathcal{A}[\phi_1\bar{\phi}_1\phi_2\bar{\phi}_2\cdots\phi_n\bar{\phi}_n]$, where $\mathcal{A}$ is the antisymmetrizer. Let the indices $i,j,k,\ldots$ refer to the occupied HF MOs $\{\phi_i\}$ and $u,v,w,\ldots$ to unoccupied HF MOs. All the HF MOs are determined by diagonalizing the one electron HF operator ${}^1F$,

$$ {}^1F_{lm} = \langle\phi_l|H + \sum_{k=1}^{\text{occ}}(2J_k - K_k)|\phi_m\rangle = \delta_{lm}\epsilon_l, \tag{1}$$

where l and m designate any (occupied or unoccupied) HF MO and ϵ_l is the HF orbital energy. The operator H is the one-electron portion of the Hamiltonian, and J_k and K_k are Coulomb and exchange operators, respectively, for the occupied orbital ϕ_k.

An excited state HF computation would provide a new set $\{\chi\}$ of MOs that produce the lowest possible energies for the low lying singly excited $\Psi_{\alpha\to\mu}$ state,

$$\Psi(\alpha\to\mu) = \mathcal{A}[\chi_1\bar{\chi}_1\chi_2\bar{\chi}_2\cdots(\chi_\alpha\bar{\chi}_\mu \pm \chi_\mu\bar{\chi}_\alpha)\cdots\chi_n\bar{\chi}_n], \tag{2}$$

corresponding to an excitation of an electron from the orbital χ_α to χ_μ, where the + and − signs correspond to triplet and singlet states, respectively. The new MOs $\{\chi_\alpha\}$ and $\{\chi_\mu\}$ may be expressed as a linear combination of the ground state MOs $\{\phi_i,\phi_u\}$. If, however, the orbitals are restricted such that the $\{\chi_\alpha\}$ are linear combinations of only the occupied ground state MOs $\{\phi_\alpha\}$ and the $\{\chi_\mu\}$ are expanded only in terms of the unoccupied $\{\phi_u\}$,

$$\chi_\alpha = \sum_{i=1}^{\text{occ}} a_{\alpha i}\phi_i; \quad \chi_\mu = \sum_{u=1}^{\text{unocc}} c_{\mu u}\phi_u, \tag{3}$$

then the new orbital set $\{\chi_\alpha,\chi_\mu\}$ not only leaves the ground state wave function unchanged but also ensures the orthogonality and applicability of Brillouin's theorem between the HF ground state and the $\Psi_{\alpha\to\mu}$ excited states. In addition, this choice also benefits from using a common set of MOs for the ground and excited states, a choice which simplifies the computation of oscillator strengths, etc. However, we avoid the computationally laborious reoptimization of the occupied orbitals by setting $\{\chi_\alpha\}\equiv\{\phi_\alpha\}$, i.e., by choosing $a_{\alpha j} = \delta_{\alpha j}$, thereby simplifying enormously the procedure for generating the IVOs. Hence, the coupled equations determining the coefficients $a_{\alpha j}$ and $c_{\mu\nu}$ reduce to a single eigenvalue equation of the form $F'C = C\Gamma$, where the operator F' is given by

$$F'_{vw} = {}^1F_{vw} + A^\alpha_{vw}, \tag{4}$$

where ${}^1F$ is the ground state Fock operator and the additional term A^α_{vw} accounts for the excitation of an electron out of orbital ϕ_α,

$$A^\alpha_{vw} = \langle\chi_v| - J_\alpha + K_\alpha \pm K_\alpha|\chi_w\rangle. \tag{5}$$

The minus sign in Eq. (5) applies for ${}^3\Psi_{\alpha\to\mu}$ triplet state, while the plus sign is for the singlet ${}^1\Psi_{\alpha\to\mu}$ state.[26,46] The corresponding transition energy is

$${}^{1,3}\Delta E(\alpha\to\mu) = E_0 + \gamma_\mu - {}^1F_{\alpha\alpha}, \tag{6}$$

where E_0 is the HF ground state energy and γ_μ is the eigenvalue of $F'C = C\Gamma$ for the μth orbital.

Special care is required for systems where the highest occupied HF MOs are doubly degenerate. In order that the $\{\chi_\mu\}$ retain molecular symmetry, the construction of F' must be modified from Huzinaga's scheme. If ϕ_α and ϕ_β are the highest occupied degenerate HF MOs, then the matrix element A^α_{vw} in Eq. (6) is replaced for these degenerate systems by $A^{\alpha,\beta}_{vw}$, where

$$A^{\alpha,\beta}_{vw} = \tfrac{1}{2}\langle\chi_v| - J_\alpha + K_\alpha \pm K_\alpha|\chi_w\rangle + \tfrac{1}{2}\langle\chi_v| - J_\beta + K_\beta \pm K_\beta|\chi_w\rangle. \tag{7}$$

B. Formal structure of the first order energy gradients

Before presenting the formal structure of the first derivatives of the electronic energy, we emphasize that the working equations for the energy gradients have been discussed at length by several pioneers in this field.[1,5,44,47] Our working approach for evaluating the first derivatives of the electronic energy is closely related to the one summarized by Yamaguchi *et al.*[44] in their review article, so some details from their approach are omitted for brevity.

Let $\Psi^I(r,R)$ be the CASCI eigenfunction of the nonrelativistic Born–Oppenheimer Hamiltonian $H_{\text{elec}}(r,R)$ for a system of n-electrons and N-nuclei in the space of the zeroth order reference functions $\Phi_K(r,R), K=1,\ldots,M$, i.e.,

$$H_{\text{elec}}(r,R)\Psi^I(r,R) = E^I_{\text{elec}}(R)\Psi^I(r,R), \tag{8}$$

where r and R are the electron and nuclear coordinates, respectively, and where $\Psi_I(r,R)$ is given by

$$\Psi^I(r,R) = \sum_I^M C_I(R)\Phi_I(r,R), \tag{9}$$

with

$$\sum_I^M C_I^2(R) = 1. \tag{10}$$

The $\Phi_k(r,R)$ are symmetry adapted CSFs and $C^I(R)$ are the corresponding CI coefficients. The CSFs $\Phi^I(r,R)$ can be expressed in terms of Slater determinants containing orthonormal MOs $\phi_k(r,R)$,

$$\Phi^I(r,R) = \sum_k m^k_\lambda \frac{1}{\sqrt{N!}}\sum_P^{N!}(-1)^P P[\phi_1(1)\phi_2(2)\cdots\phi_k(N)], \tag{11}$$

where P is a permutation operator and m^k_λ are the Clebsch–Gordan coefficients. Further, the MOs can be written as linear combinations of atom centered basis functions (AOs) $\chi_l(r,R)$,

$$\phi_i(r,R) = \sum_{\mu}^{\mathrm{AO}} t_{\mu}^{i}(R)\chi_{\mu}(r,R), \tag{12}$$

where $t_{\mu}^{i}(R)$ are the MO expansion coefficients. The MOs $\phi(r,R)$ are chosen to be orthonormal, i.e.,

$$S_{ij} = \langle \phi_i(r,R) | \phi_j(r,R) \rangle = \delta_{ij}. \tag{13}$$

The electronic energy E_{elec} corresponding to a CI wave function is given by

$$E_{\mathrm{elec}} = \sum_{IJ}^{\mathrm{CI}} C_I C_J \langle \Phi_I | H_{\mathrm{elec}} | \phi_J \rangle = \sum_{IJ}^{\mathrm{CI}} C_I C_J H_{IJ}, \tag{14}$$

where the Born–Oppenheimer Hamiltonian H_{elec} for n electrons and N nuclei is

$$H_{\mathrm{elec}} = -\sum_{i}^{n}\left[\frac{1}{2}\nabla_i^2 + \sum_{A}^{N}\frac{Z_A}{r_{iA}}\right] + \sum_{i>j}^{n}\frac{1}{r_{ij}} = \sum_{i}^{n} h(i) + \sum_{i>j}^{n}\frac{1}{r_{ij}}, \tag{15}$$

in which Z is the nuclear charge and $h(i)$ the usual one-electron operator,

$$h(i) = -\sum_{i}^{n}\frac{1}{2}\nabla_i^2 - \sum_{i}^{n}\sum_{A}^{N}\frac{Z_A}{r_{iA}}. \tag{16}$$

The total energy E_{tot} of the system is then given by

$$E_{\mathrm{tot}} = E_{\mathrm{elec}} + \sum_{A>B}^{N}\frac{Z_A Z_B}{R_{AB}}, \tag{17}$$

where R_{AB} is an internuclear separation.

Differentiating Eq. (14) with respect to nuclear coordinate R yields

$$\frac{\partial E_{\mathrm{elec}}}{\partial R} = \sum_{IJ}^{CI}\left[\frac{\partial C_I}{\partial R}C_J H_{IJ} + C_I\frac{\partial C_J}{\partial R}H_{IJ} + C_I C_J\frac{\partial H_{IJ}}{\partial R}\right], \tag{18}$$

which can be further written as

$$\frac{\partial E_{\mathrm{elec}}}{\partial R} = 2\sum_{IJ}^{CI}\frac{\partial C_I}{\partial R}H_{IJ}C_J + \sum_{IJ}^{CI} C_I C_J\frac{\partial H_{IJ}}{\partial R} \tag{19}$$

by interchanging summation indices. Invoking the variational condition within the CI space, i.e., $\Sigma_J H_{IJ}C_J = E_{\mathrm{elec}}C_I$, Eq. (19) can be further expressed as

$$\frac{\partial E_{\mathrm{elec}}}{\partial R} = 2E_{\mathrm{elec}}\sum_{I}^{\mathrm{CI}}\frac{\partial C_I}{\partial R}C_I + \sum_{IJ}^{\mathrm{CI}} C_I C_J\frac{\partial H_{IJ}}{\partial R}, \tag{20}$$

or simply

$$\frac{\partial E_{\mathrm{elec}}}{\partial R} = \sum_{IJ}^{\mathrm{CI}} C_I C_J\frac{\partial H_{IJ}}{\partial R} \tag{21}$$

because of the normalization condition

$$\sum_{I}^{\mathrm{CI}}\frac{\partial C_I}{\partial R}C_I = 0. \tag{22}$$

Now, the matrix elements of Hamiltonian H_{elec} with respect to the CSFs I and J are written as the form[44]

$$H_{IJ} = \sum_{ij}^{\mathrm{MO}}\gamma_{ij}^{IJ}h_{ij} + \sum_{ijkl}^{\mathrm{MO}}\Gamma_{ijkl}^{IJ}(ij|kl), \tag{23}$$

where γ_{ij}^{IJ} and Γ_{ijkl}^{IJ} are the one- and two-particle transition density matrices, and the one- and two-electron MO integrals h_{ij} and $(ij|kl)$ are given by

$$h_{ij} = \int \phi_i^*(1)h(1)\phi_j^*(1)d\tau_1 \tag{24}$$

and

$$(ij|kl) = \int\int \phi_i^*(1)\phi_j^*(1)\frac{1}{r_{12}}\phi_k^*(2)\phi_l^*(2)d\tau_1 d\tau_2, \tag{25}$$

respectively. Here, the choice of orbitals remains quite general and can be assumed to comprise HF orbitals for the occupied orbitals in the reference wave function and IVOs for the remaining orbitals. Substituting Eq. (23) in Eq. (14), we get

$$\frac{\partial E_{\mathrm{elec}}}{\partial R} = \sum_{IJ}^{\mathrm{CI}} C_I C_J\left[\sum_{ij}^{\mathrm{MO}}\gamma_{ij}^{IJ}\frac{\partial h_{ij}}{\partial R} + \sum_{ijkl}^{\mathrm{MO}}\Gamma_{ijkl}^{IJ}\frac{\partial (ij|kl)}{\partial R}\right]. \tag{26}$$

Now, defining the full one- and two-particle reduced density matrices as

$$\gamma_{ij} = \sum_{ij}^{\mathrm{MO}} C_I C_J\gamma_{ij}^{IJ}, \quad \Gamma_{ijkl} = \sum_{ijkl}^{\mathrm{MO}} C_I C_J\Gamma_{ijkl}^{IJ}, \tag{27}$$

respectively, we can rewrite Eq. (26) as

$$\frac{\partial E_{\mathrm{elec}}}{\partial R} = \sum_{ij}^{\mathrm{MO}}\gamma_{ij}\frac{\partial h_{ij}}{\partial R} + \sum_{ijkl}^{\mathrm{MO}}\Gamma_{ijkl}\frac{\partial (ij|kl)}{\partial R}. \tag{28}$$

The derivatives of the one-electron MO integrals appearing in Eqs. (26) and (28) can be represented as

$$\frac{\partial h_{ij}}{\partial R} = \frac{\partial}{\partial R}\sum_{\mu\nu}^{\mathrm{AO}} t_{\mu}^{i}t_{\nu}^{j}h_{\mu\nu} = \sum_{\mu\nu}^{\mathrm{AO}}\left[\frac{\partial t_{\mu}^{i}}{\partial R}t_{\nu}^{j}h_{\mu\nu} + t_{\mu}^{i}\frac{\partial t_{\nu}^{j}}{\partial R}h_{\mu\nu} + t_{\mu}^{i}t_{\nu}^{j}\frac{\partial h_{\mu\nu}}{\partial R}\right]. \tag{29}$$

Expressing the μth perturbed MO coefficients in terms of the perturbation parameter λ as

$$t_{\mu}^{i^{\mathrm{pert}}} = t_{\mu}^{i} + \lambda\sum_{m}^{\mathrm{MO}}\frac{\partial t_{\mu}^{i}}{\partial R} + \cdots = t_{\mu}^{i} + \lambda\sum_{m}^{\mathrm{MO}} U_{mi}^{R}t_{\mu}^{M} + \cdots, \tag{30}$$

where U_{mi}^{R} denotes the changes in the MO coefficients of the μ th orbital (molecular) due to nuclear perturbation and is defined as

$$\frac{\partial t_{\mu}^{i}}{\partial R} = \sum_{m}^{\mathrm{MO}} U_{mi}^{R}t_{\mu}^{m}. \tag{31}$$

Substituting Eq. (31) in Eq. (29), we get

$$\frac{\partial h_{ij}}{\partial R} = h_{ij}^R + \sum_m^{\mathrm{MO}} [U_{mi}^R h_{mj} + h_{im} U_{mj}^R], \tag{32}$$

where the superscript R indicates the derivative with respect to R. Likewise, the derivatives of two-electron MO integrals are obtained as

$$\frac{\partial (ij|kl)}{\partial R} = (ij|kl)^R + \sum_m^{\mathrm{MO}} [U_{mi}^R (mj|kl) + U_{mj}^R (im|kl) + (ij|ml) U_{mk}^R + (ij|km) U_{ml}^R]. \tag{33}$$

Substituting Eqs. (32) and (33) in Eq. (28) and performing some algebraic manipulations reduces these equations to

$$\frac{\partial E_{\mathrm{elec}}}{\partial R} = \sum_{ij}^{\mathrm{MO}} \gamma_{ij} h_{ij}^R + \sum_{ijkl}^{\mathrm{MO}} \Gamma_{ijkl} (ij|kl)^R + 2 \sum_{ij}^{\mathrm{MO}} U_{ij}^R X_{ij}, \tag{34}$$

where the Lagrangian matrix X in Eq. (34) is defined as

$$X_{ij} = \sum_m^{\mathrm{MO}} \gamma_{jm} h_{im} + 2 \sum_{mkl}^{\mathrm{MO}} \Gamma_{jmkl} (im|kl). \tag{35}$$

It is obvious from Eq. (34) that the evaluation of the first derivative of the CI energy requires the explicit evaluation of the derivatives of the MO coefficients U_{ij}^R, which are of the form (neglecting the CI derivative)

$$U_{ij}^R = \frac{F_{ij}^R - S_{ij}^R}{\epsilon_i - \epsilon_j}, \tag{36}$$

where F^R and S^R are the derivatives of Fock operator (HF or IVO) defining the MOs and of the overlap operator in the MO basis, and ϵ are the orbital energies.

Now, when the orbitals are generated from variationally optimized procedures, such as the MCSCF or the closely related IVO-CASCI methods, the Lagrangian matrix satisfies the symmetry condition, i.e.,

$$X_{ij} = X_{ji}. \tag{37}$$

The Lagrangian matrix X is related to IVO-CASCI/MCSCF Fock matrix via

$$X_{ij} = \langle \phi_i | \sum_m^{\mathrm{MO}} F_{jm} | \phi_m \rangle, \tag{38}$$

where

$$F_{ij} = \gamma_{ij} h + 2 \sum_m^{\mathrm{MO}} \Gamma_{ijkl} J_{kl}, \tag{39}$$

in which h is the one-electron operator and the two-electron operator J_{kl} satisfies

$$\langle \phi_i | J_{kl} | \phi_j \rangle = (ij|kl). \tag{40}$$

A similar symmetry condition is also used in the evaluation of the first derivatives of the energy gradient in the closed and restricted open-shell HF methods. Using the Lagrangian symmetry condition, Eq. (34) is rewritten as

$$\frac{\partial E_{\mathrm{elec}}}{\partial R} = \sum_{ij}^{\mathrm{MO}} \gamma_{ij} h_{ij}^R + \sum_{ijkl}^{\mathrm{MO}} \Gamma_{ijkl} (ij|kl)^R + \sum_{ij}^{\mathrm{MO}} (U_{ij}^R + U_{ji}^R) X_{ij}, \tag{41}$$

which can be further simplified to

$$\frac{\partial E_{\mathrm{elec}}}{\partial R} = \sum_{ij}^{\mathrm{MO}} \gamma_{ij} h_{ij}^R + \sum_{ijkl}^{\mathrm{MO}} \Gamma_{ijkl} (ij|kl)^R - \sum_{ij}^{\mathrm{MO}} S_{ij}^R X_{ij} \tag{42}$$

by invoking the orthonormality condition, i.e., $S_{ij}^R + U_{ij}^R + U_{ji}^R = 0$. Equation (42) clearly shows that the evaluation of the first derivative of the IVO-CASCI/MCSCF energy can be accomplished without the explicit computation of the U^R and $\partial C / \partial R$ derivatives. On the other hand, the computation of the second derivative of the IVO-CASCI/MCSCF energy requires the explicit evaluation of first derivatives of the MO and CI coefficients. This computation is accomplished in the MCSCF method by differentiating Eq. (37) to produce the CPMCHF equations. The detailed derivation of the CPMCHF equations for multi-Fock operator methods is sketched in Ref. 43, and the modified form used here will be presented in a future communication.

III. NUMERICAL APPLICATIONS

This section illustrates the numerical performance of our computationally inexpensive analytical gradient based IVO-CASCI method, which is completely general and easily portable to the study of very different chemical systems. The main focus of the applications is to provide high level quantum chemical calculations of geometries and vibrational frequency for some chemically interesting and challenging systems and thereby demonstrate the feasibility and efficacy of the IVO-CASCI method. Thus, we have applied this analytical gradient scheme to the benzene, biphenyl, and alanine dipeptide molecules. All the harmonic vibrational frequencies reported here are calculated using our analytic second derivative method.

Unless otherwise mentioned, all the calculations are performed using the GAMESS quantum chemistry software,[48] which has been interfaced with our IVO-CASCI module for generating improved virtual orbitals and which will be made available for distribution.

A. Benzene

We begin by examining the ground and excited state geometries and vibrational frequencies of benzene, one of the most extensively studied π-electron aromatic hydrocarbons in quantum chemistry for which the theoretical description of the ground and excited of this system is difficult due to their multireference character even in the equilibrium regions. This six-membered ring system, and particularly its S_0 and S_1 states, is of fundamental importance in spectroscopy. Extensive experimental studies of the S_0 and S_1 vibrational modes are also well documented,[49–56] and several calculations are available for the S_0 and S_1 state harmonic force fields and vibrational spectra.[57–63] Recent advances in high resolution spectroscopy have enabled the assignment of the S_0 and S_1 state vibrational frequencies of benzene more pre-

TABLE I. Optimized and experimental geometries for the ground ($X\ ^1A_g$), first excited singlet ($1\ ^1B_{2u}$), and triplet ($1\ ^3B_{1u}$) states of benzene from theories using the cc-pVDZ basis set. The bond angles and bond distances are given in degrees and angstrom, respectively.

State	Method	r_e(C–C)/Å	r_e(C–H)/Å	ΔE(kcal/mol)[a]	CPU (s)[b]
$X\ ^1A_g(S_0)$	HF	1.389	1.082		14
	MP2	1.406	1.095		32
	DFT/B3LYP	1.398	1.093		43
	CASSCF	1.398	1.082		65[c], 34[d]
	IVO-CASCI	1.398	1.082		14
	Expt.	1.397[e]	1.084[e]		
$1\ ^1B_{2u}$	CASSCF	1.436	1.080	110	20[c], 34[d]
	IVO-CASCI	1.436	1.080	110	33
	Expt.	1.435[f]	1.070[f]	113[g]	
$1\ ^3B_{1u}$	CASSCF	1.432	1.080	85	67[c]
	IVO-CASCI	1.432	1.080	85	33
	Expt.			90[h]	

[a]$E_{\text{CASSCF/IVO-CASCI}}(X\ ^1A_g) = -230.794\ 31$ a.u.
[b]CPU time for single energy+gradient calculation.
[c]From GAMESS package (Ref. 48).
[d]From DALTON package (Ref. 65).
[e]Reference 66.
[f]Reference 49.
[g]Reference 67.
[h]Reference 68.

cisely and, therefore, a rigorous comparison between theory and experiment provides a stringent assessment for the accuracy of *ab initio* many-body methods.

The geometry optimizations for the ground $X\ ^1A_g(S_0)$ and first excited singlet $^1B_{2u}(S_1)$ and triplet $^3B_{1u}$ states of benzene are performed with the correlation consistent polarized-valence double-ζ (cc-pVDZ) Dunning basis set[64] without altering the active space. The calculations assume a D_{2h} (subgroup of D_{6h}) point group symmetry for convenience in checking for possible symmetry lowering. The active space in these calculations comprises three bonding valence π orbitals (b_{2u}, b_{1g}, and b_{3g}) and three antibonding valence π^* orbitals (b_{3g}, b_{2u}, and a_u). Consequently, the active space used in IVO-CASCI calculations contains 51 and 52 CSFs for the treatment of the $^3B_{1u}$ and $X\ ^1A_g$ states, respectively.

The ground state geometry determined from HF, MP2, density functional theory (DFT)/B3LYP, CASSCF, and IVO-CASCI calculations exhibits some striking differences (see Table I) in the computed C–C and C–H bond lengths, namely, (a) the HF calculations yield the C–C and C–H bonds as 0.008 and 0.002 Å shorter than the experiment, whereas the DFT/B3LYP procedure estimates these bonds to be 0.002 and 0.011 Å longer than the observed values;[66] (b) the MP2 predicted C–C and C–H bond lengths are off by 0.009 Å from the experiment; (c) the C–C and C–H bond lengths from the IVO-CASCI and CASSCF methods are accurate to 0.001 and 0.002 Å, respectively. It is pertinent to note that the CPU times elapsed during the IVO-CASCI and CASSCF geometry optimization are 189 and 367 s, respectively, a difference which mainly arises because of the need for a CASSCF iteration cycle at each intermediate geometry.

Since the first excited singlet $^1B_{2u}(S_1)$ state of benzene is an open shell, the geometry optimizations are determined only at the IVO-CASCI and CASSCF level. As shown in Table I, the C–C bond length increases from 1.397 to 1.435 Å during the $S_0 \rightarrow S_1$ excitation, while the C–H bond length decreases from 1.086 to 1.070 Å. These changes in bond lengths are consistent with other theoretical estimates. Table I also exhibits the IVO-CASCI estimates of the C–C and C–H bond lengths for the S_1 state as deviating by only 0.001 and 0.01 Å, respectively, from the experiment.[49] The geometries reported in Table I for the S_0 and S_1 states further indicate that the D_{6h} point group symmetry is preserved during the optimization procedure. The lack of lowering of the symmetry in the transition between the S_0 and S_1 states agrees with the experimentally observed selection rules.

The geometry of benzene in its lowest triplet state ($^3B_{1u}$) has been a subject of several experimental and theoretical investigations[69,70] since the $^3B_{1u}$ state exhibits conformational instability due to strong vibronic coupling with the $^3E_{1u}$ state through e_{2g} modes. Theoretical calculations of the vibronic coupling support this interpretation of the spectroscopic results.[71] We compute the geometry and vibrational frequencies of the $1\ ^3B_{1u}$ state using the CASSCF and IVO-CASSCI schemes to analyze the stability of these states. Table I presents the optimized molecular dimensions and adiabatic transition energy from the ground $X\ ^1A_g$ state as determined with the CASSCF and IVO-CASCI methods. The calculated bond lengths and bond angles demonstrate

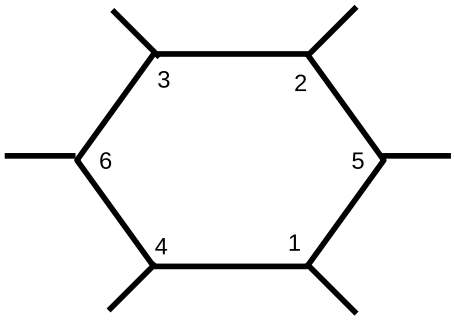

FIG. 1. Labeling of molecular structure for the triplet states of benzene.

TABLE II. Optimized triplet state geometries of benzene. Bond distances, bond angle, energy with respect to ground state, and CPU time are in angstrom, degrees, kcal/mol, and seconds.

State	Parameters	IVO-CASCI[a]	CASSCF[b]	Expt.
$^3A_1$				
	$r_e(C1-C4)=r_e(C2-C3)$	1.3628	1.3628	
	$r_e(C1-C5)=r_e(C2-C5)=r_e(C4-C6)=r_e(C3-C6)$	1.4698	1.4698	
	$r_e(C1-H)=r_e(C2-H)=r_e(C3-H)=r_e(C4-H)$	1.0816	1.0816	
	$r_e(C5-H)=r_e(C6-H)$	1.0787	1.0787	
	$\angle C4-C1-C5=\angle C3-C2-C5=\angle C2-C3-C6$ $=\angle C1-C4-C6$	120.51	120.51	
	$E(1\ ^3A_1)-E(X\ ^1A_g)$	82	82	90[c]
	CPU[d]	22	43	
$^3B_1$				
	$r_e(C1-C4)=r_e(C2-C3)$	1.4372	1.4372	
	$r_e(C1-C5)=r_e(C2-C5)=r_e(C4-C6)=r_e(C3-C6)$	1.4293	1.4293	
	$r_e(C1-H)=r_e(C2-H)=r_e(C3-H)=r_e(C4-H)$	1.0799	1.0799	
	$r_e(C5-H)=r_e(C6-H)$	1.0807	1.0807	
	$\angle C4-C1-C5=\angle C3-C2-C5=\angle C2-C3-C6$ $=\angle C1-C4-C6$	119.68	119.68	
	$E(1\ ^3B_1)-E(X\ ^1A_g)$	111	111	
	CPU[d]	22	43	

[a] $E_{CASSCF/IVO-CASCI}(X\ ^1A_g)=-230.794\ 31$ a.u.
[b] From DALTON package.
[c] Reference 68.
[d] CPU time for single energy+gradient calculation.

that the hexagonal molecular structure (D_{6h}) is preserved during the optimization procedure. In passing, we note that the CASSCF geometry obtained using the DALTON package[65] yields a lower symmetry (D_{2h}) solution for the $^3B_{1u}$ and $^1B_{2u}$ states.

Interestingly, the calculations at C_{2v} symmetry (subgroup of D_{2h}) yield two stable triplet states. The ground state configuration of benzene under C_{2v} symmetry is $11a_1^2 7b_1^2 2b_2^2 1a_2^2$. The triplet state geometry optimization is carried out with a $[(1-4)b_2(1-2)a_2]^6$ CAS space (3π and

TABLE III. Comparison of calculated and experimental vibrational frequencies (in cm^{-1}) of ground ($X\ ^1A_g/S_0$) and first excited singlet ($1\ ^1B_{2u}/S_1$) state of benzene. [Entries are the differences with respect to experiment (theory experiment).]

	$X\ ^1A_g$				$1\ ^1B_{2u}$		
Symmetry	HF	IVO-CASCI	CASSCF	Expt.[a]	IVO-CASCI	CIS[b]	Expt.[c]
a_{1g}	297	292	291	3074	256	287	3130
	88	50	46	993	36	114	923
a_{2g}	94	86	86	1350	198	273	1246
b_{1u}	271	267	267	3057	190	216	3159
	76	79	79	1010	122	181	936
b_{2u}	33	19	19	1309	286	278	1570
	39	30	30	1150	92	159	1148
e_{2g}	282	277	277	3057	280	305	3077
	175	118	118	1601	207	281	1454
	95	79	79	1178	80	152	1148
	53	42	42	608	56	79	522
e_{1u}	295	290	290	3064	291	321	3081
	123	102	102	1484	114	207	1401
	93	68	68	1038	42	159	919
a_{2u}	79	31	32	674	15	166	515
b_{2g}	127	31	31	990	−47	227	749
	64	13	12	707	130	27	365
e_{1g}	102	19	20	847	12	156	585
e_{2u}	123	18	19	967	−37	213	713
	52	31	31	398	62	58	237
Deviation (rms)	154	137	137		158	209	

[a] See Ref. 53 for experimental references.
[b] Reference 57.
[c] Reference 54.

TABLE IV. Calculated harmonic vibrational frequencies (in cm^{-1}) for the first excited $1\ ^3A_1$ and $1\ ^3B_1$ states of benzene.

	$1\ ^3A_1$		$1\ ^3B_1$	
Symmetry	CASSCF[a]	IVO-CASCI	CASSCF[a]	IVO-CASCI
a_1	3387	3387	3386	3385
	3379	3379	3369	3368
	3353	3353	3351	3350
	3335	3335	3348	3347
	1599	1598	1660	1659
	1504	1503	1509	1509
	1219	1220	1226	1226
	1064	1064	1066	1067
	956	956	972	987
	857	856	932	931
	579	579	553	553
b_1	3359	3359	3373	3372
	3336	3336	3368	3367
	1642	1642	2311	2310
	1497	1497	1606	1605
	1444	1444	1447	1445
	1391	1391	1392	1392
	1236	1236	1303	1302
	1069	1069	1232	1231
	755	754	801	800
	489	488	575	572
b_2	906	905	749	747
	681	681	745	743
	512	512	631	630
	249	247	555	554
	243	240	492	501
	155	152	312	291
a_2	902	901	682	681
	674	673	609	606
	385	384	289	291

[a]From DALTON package.

TABLE V. Calculated vibrational frequencies (in cm^{-1}) for the first excited triplet ($1\ ^3B_{1u}$) state of benzene at the saddle point (D_{6h}) and at the (D_{2h}) minima along the internal reaction coordinate (Fig. 2).

Symmetry	Saddle point	Minima
a_g	3381	3373
	3348	3212
	1353	1613
	956	1238
	628	960
	1469*i*	586
b_{3u}	3369	3213
	1547	1653
	1526	1500
	1235	1264
	971	1071
b_{2u}	701	770
	549	259
	312	186
b_{1g}	617	718
b_{1u}	3369	3369
	3345	3188
	1526	1531
	1073	1063
	971	870
b_{2g}	3348	3188
	1449	1453
	1353	1396
	628	760
	1469*i*	485
b_{3g}	730	959
	617	509
	514	250
a_u	701	968
	312	385

$3\pi^*$ orbitals) and the computed molecular dimensions (Fig. 1) are summarized in Table II. Thus, the active space employed in these calculations contains 93 and 96 CSFs for the treatment of the $^3A_1$ and $^3B_1$ states, respectively.

The structural parameters displayed in Table II reveal that the C1–C4 and C2–C3 bond distances in $^3B_1$ differ by only 0.008 Å from the other four C–C bond lengths. Likewise, we find that the C5–H and C6–H bond lengths in $^3B_1$ are also relatively close (differ by 0.0008 Å) to the other four C–H bond lengths. But the picture is completely different for the $^3A_1$ state where the C1–C4 and C2–C3 bond lengths differ by 0.107 Å from the other C–C bonds, and the C5–H and C6–H bonds deviate by 0.003 Å from the other four C–H bonds. While the C–C bond lengths in the $^3A_1$ and $^3B_1$ states differ substantially, the C–C–C bond angles differ only by 1°.

The benzene ground (S_0) and first excited states (S_1) have 30 fundamentals with symmetries $2a_{1g}+a_{2g}+2b_{1u}+2b_{2u}+2b_{2g}+a_{2u}+3e_{1u}+2e_{2u}+4e_{2g}+e_{1g}$ for their D_{6h} structures. The normal mode frequencies of the S_0 and S_1 states are computed with the HF, CASSCF, and IVO-CASCI methods and are compared with the experiment[51–54,56] in Table III. The computed normal mode frequencies are all *real*, implying that the optimized geometries are at *minima*. A relatively good agreement emerges between the calculated vibrational spectra for the S_0 and S_1 states from the IVO-CASCI and CASSCF methods. The root-mean-square (rms) deviations between the calculated IVO-CASCI and observed frequencies are 137 and 158 cm^{-1} for the S_0 and S_1 states, respectively. The maximum deviations in our calculated vibrational frequencies are 292 cm^{-1} (a_{1g}) and 291 cm^{-1} (e_{1u}) for the S_0 and S_1 states, respectively.

The CASSCF and IVO-CASCI harmonic vibrational frequencies for the triplet states of benzene are displayed in Table IV for all 30 fundamentals with symmetries $11a_1+10b_1+6b_2+3a_2$ for the C_{2v} structure. Since none of frequencies is imaginary, both structures are stable. The geometries and frequencies for the triplet states are determined from DALTON package to demonstrate the reliability of our proposed scheme because while the IVO-CASCI geometry optimization with GAMESS takes less time than with the DALTON package, the frequency calculation is more time consuming with GAMESS than with the DALTON package.

The vibrational frequencies for C–H stretching modes in Table III display the common characteristic of deviating by more than 200 cm^{-1} from the experiment, whereas our computed frequencies for the other modes well reproduced the

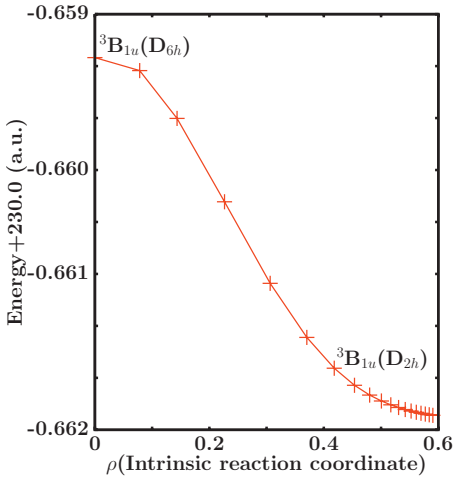

FIG. 2. Energy as a function of the distance along the reaction path in mass weighted Cartesian space. The path is along the direction of the largest magnitude of the downhill component of the imaginary normal mode.

experiment. As is well known, the frequencies obtained upon diagonalization of harmonic force fields, in general, exceed (10% on average)[57] the experiment, and, consequently, the *ab initio* vibrational frequencies are commonly scaled to reproduce the observed frequencies. For example, the CH and CC stretching frequencies for the S_0 and S_1 states are scaled by factors of 0.83 and 0.82 by Orlandi *et al.*[57] A closer analysis of the data presented in Table III shows that the difference between IVO-CASCI predicted and the experimental vibrational frequencies would also diminish if the IVO-CASCI frequencies are also scaled by 0.82. However, in order to demonstrate the accuracy and strength of the method, this scaling procedure is not introduced here.

The calculated 0-0 adiabatic energy separation between the X ^1A_g–1 $^3B_{1u}$ and X ^1A_g–1 $^1B_{2u}$ states from the IVO-CASCI and CASSCF methods is accurate to 5 and 3 kcal/mol, respectively. The present calculations estimate the X $^1A_g \rightarrow 1\ ^3B_{1u}$ and X ^1A_g–1 $^1B_{2u}$ transition energies to be 85 and 110 kcal/mol, where the corresponding experimental values are 90 and 113 kcal/mol, respectively. Thus, the data in Tables I–IV clearly demonstrate that the CASSCF and IVO-CASCI methods describe the X $^1A_g(S_0)$, 1 $^1B_{2u}(S_1)$, and 1 $^3B_{1u}$ states of benzene in a reasonably balanced fashion for the chosen active space.

The vibrational frequencies computed using the CASSCF and IVO-CASCI methods yield a pair of imaginary frequencies for the first excited triplet state of B_{1u} symmetry.

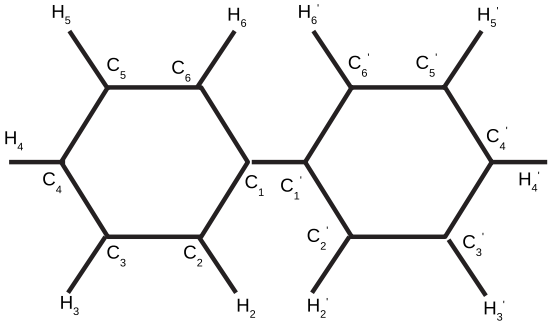

FIG. 3. Structure of coplanar biphenyl molecule.

This implies that the 1 $^3B_{1u}$ is conformationally *unstable*, a finding that is also in accord with the experiment and with earlier theoretical calculations.[69,70] In fact, Moffitt *et al.*[69] explain that the conformational instability of the 1 $^3B_{1u}$ state arises due to strong vibronic coupling between the $^3B_{1u}$ and $^3E_{1u}$ states. In order to analyze the conformational instability, our geometry optimization in D_{6h} symmetry as expected produces a saddle with a pair of imaginary frequencies (see Table V). We then employ the IRC path method to study the potential curve along the direction of the largest magnitude downhill component of the imaginary normal mode (see Fig. 2). The use of the IRC path method leads to a stable conformer of D_{2h} point group symmetry (see Table V). Finally, it is important to emphasize that the IVO-CASCI treatment yields almost identical results to the CASSCF scheme at a fraction of the computational cost (see Tables I and II). Thus, the IVO-CASCI procedure is a viable replacement for the CASSCF method.

B. Biphenyl

Another system of great interest is the biphenyl molecule (H_5C_6–C_6H_5) owing, in part, to the nonrigid geometry and conformational changes during electronic excitation. The study of biphenyl also helps in understanding the interaction between two subsystems, two benzene molecules. The accurate determination of the thermodynamic properties of biphenyl is also of great importance because biphenyl is an environmentally significant compound. Consequently, the geometry, vibrational frequencies, and internal rotational potential of the biphenyl molecule have long been the subject of theoretical[72–80] and experimental[78,81–89] study in spite of the difficulty of *ab initio* calculations because of its size. However, some experimental and theoretical findings exhibit inconsistencies, which should be resolved through more accurate calculations. While it is desirable to investigate the geometries of the biphenyl conformers and their relative stability with high level *ab initio* methods, the size of the system has usually prevented or at lest attenuated the calculations before reaching the *ab initio* limit.

The molecular structure of biphenyl (Fig. 3) is mainly characterized by the twisting angle (ϕ) between the two phenyl rings because this angle strongly depends on the state of aggregation. For example, the experimental data for biphenyl in the solid state are consistent with a coplanar structure (ϕ=0), whereas gas phase electron diffraction experiments indicate that a nonplanar (ϕ=44.3°+±1.3°) structure is energetically more stable.

The first *ab initio* geometry optimization of biphenyl by Almlöf uses HF calculations and a double-ζ quality basis. Almlöf demonstrates that the nonplanar structure (ϕ=32°) is energetically most stable. The rotational barrier heights E_ϕ reported in his calculations are 5.0 and 18.9 kJ/mol for the planar (ϕ=0) and perpendicular (ϕ=90) conformers, respectively. Several subsequent theoretical calculations employ different approaches to locate the most stable structure and its stability. For example, the rotational barrier heights E_0 and E_{90} from HF and MP2 calculations lie in the range of 13–16 and 5–7 kJ/mol, whereas the electron diffraction study

TABLE VI. Computed equilibrium geometry of biphenyl molecule from 6-31G* basis set calculations. The bond angles, bond distances, and energies are given in degrees, angstrom, and a.u., respectively.

Parameters	HF	MP2	IVO-CASCI	DFT	Expt.[a]
ϕ [b]	44.6	46.4	44.2	39.0	44.4
C_1-C_1'	1.489	1.492	1.490	1.488	1.507
C_1-C_2	1.395	1.419	1.405	1.410	1.404
C_2-C_3	1.387	1.411	1.397	1.398	1.395
C_3-C_4	1.387	1.413	1.398	1.400	1.396
C_2-H_2	1.073	1.093	1.074	1.086	1.102
C_3-H_3	1.073	1.091	1.074	1.086	
C_4-H_4	1.073	1.091	1.073	1.086	
$\angle C_2-C_1-C_6$	118.4	118.7	118.3	118.2	119.4
$\angle C_1-C_2-C_3$	120.8	120.7	120.9	120.9	119.9
$\angle C_2-C_3-C_4$	120.2	120.2	120.3	120.3	
$\angle C_3-C_4-C_5$	119.5	119.6	119.4	119.5	
$\angle C_1-C_2-H_2$	119.5	119.4	119.6	119.5	
$\angle C_2-C_3-H_3$	119.7	119.8	119.7	119.7	
$\angle C_3-C_4-H_4$	120.3	120.2	120.3	120.3	
Energy[c]	−0.095 86	−1.1347	−0.2483	−2.9023	

[a]Reference 83.
[b]$C_2-C_1-C_1'-C_2'$ dihedral angle.
[c]Energy=ground state energy+460.0.

suggests these gaps to be 6.0 ± 2.1 and 6.5 ± 2.0 kJ/mol, respectively. The twisting angle reported in these calculations varies from 38.6° to 46.3°, a range which is quite substantial. Thus, one aim of the present work is to provide an accurate estimate of the barrier heights and geometries of the biphenyl conformers.

The geometry optimizations of the coplanar (D_{2h}), twisted (D_2), and perpendicular (D_{2d}) conformations are effected with HF, MP2, DFT, and IVO-CASCI methods using the 6-31G* and polarization consistent (pc) basis sets. Actual calculations, for convenience, are performed with D_2 symmetry (a subgroup of $D_{2h/2d}$). The active space for the IVO-CASCI calculations is constructed by allocating 12 valence π-electrons over 12 valence π-MOs in all possible ways to yield 57 008 CSFs. For the coplanar geometry, these 12 π-valence orbitals are of b_{1u} (4), b_{2g} (4), b_{3g} (2), and a_u (2) symmetries, where the entrees within parentheses indicate the number of MOs present in the active space.

1. Twisted geometry (D_2)

This twisted geometry (which reduces the symmetry from point group D_{2h} to D_2) represents a wide class of chemically important issues such as the description of transition states and diradicals. As the twisting angle increases, no coupling between the excited states is introduced, and thus no new states are generated. The geometries of the nonplanar conformer from HF, MP2, DFT, and IVO-CASCI calculations with the 6-31G* Gaussian basis set (128 basis functions) are compared with the experiment[83] in Table VI which exhibits some noticeable differences in the computed C–C and C–H bond lengths and the torsional angle: (a) the HF optimized geometries agree reasonably well with the experiment except for the C–H, C_2-C_3, and C_3-C_4 bonds, (b) MP2 calculations overestimate the C–C bond lengths of the phenyl ring by ~0.02 Å and the torsional angle by 2°, (c) the IVO-CASCI approach yields shorter C–H bonds, and (d) the torsional angle estimated from DFT deviates by 5.4° from the experiment.

The accuracy of the C–C and C–H bond lengths, however, improves significantly when the geometry optimizations are performed with Jensen's pc basis set[90] augmented with one polarization function.[90] The contraction schemes used in the pc-1 basis set for hydrogen and carbon atoms are [4s1p]/(2s1p) and [11s4p1d]/(3s2p1d), respectively. The geometries obtained from this basis set for the twisted geometry clearly demonstrate a significant improvement (see Table VII) especially for the HF and DFT procedures. However, this is perhaps fortuitous as the coplanar treatments (discussed below) do not exhibit any such trend.

2. Coplanar geometry (D_{2h})

Tables VIII and IX, respectively, compare the geometry of the coplanar conformer, as determined from HF, MP2, DFT, and IVO-CASCI calculations using the 6-31G* (128 basis functions) and pc-1 basis sets (218 basis functions) with the experiment.[82] Table VIII demonstrates that the optimized geometries from all these scheme are reasonably accurate, but the error in the computed barrier height differs significantly. For example, the barrier height at 0° from HF, MP2, DFT, and IVO-CASCI calculations deviates by 7.6, 11.4, 4.0, and 5.7 kJ/mol, respectively. The results from the pc-1 basis set also exhibit very similar trends, except (a) the error in the MP2 optimized $C_1-C_1^{\alpha}$, C_1-C_2, C_2-C_3, and C_3-C_4 bond distances reduces to 0.006, 0.012, 0.007, and 0.011 Å from 0.01, 0.026, 0.022, and 0.026 Å, and (b) the error in the IVO-CASCI optimized C_1-C_2, C_2-C_3, and C_3-C_4 bond distances reduces to 0.002, 0.005, and 0.003 Å from 0.012, 0.008, and 0.011 Å. In passing, we note that the IVO-CASCI and CASSCF geometry optimizations require 385 and 1012 s, respectively.

TABLE VII. Calculated equilibrium geometry for the twisted biphenyl molecule from the pc-1 basis set (except for the CASSCF) calculation. The bond angles, bond distances, and energy are given in degrees, angstrom, and a.u., respectively.

Parameters	HF	MP2	CASSCF[a,b]	IVO-CASCI	DFT	Expt.[c]
ϕ	44.9	50.4	44.3	45.2	44.7	44.4
C_1-C_1'	1.489	1.479	1.492	1.488	1.487	1.507
C_1-C_2	1.391	1.404	1.409	1.400	1.405	1.404
C_2-C_3	1.384	1.396	1.399	1.394	1.394	1.395
C_3-C_4	1.383	1.397	1.399	1.393	1.396	1.396
C_2-H_2	1.076	1.088	1.077	1.077	1.090	1.102
C_3-H_3	1.077	1.088	1.077	1.078	1.090	
C_4-H_4	1.077	1.087	1.077	1.077	1.090	
$\angle C_2-C_1-C_6$	118.2	119.0	118.4	118.3	118.2	119.4
$\angle C_1-C_2-C_3$	121.0	120.5	120.9	120.9	120.9	119.9
$\angle C_2-C_3-C_4$	120.2	120.2	120.2	120.2	120.3	
$\angle C_3-C_4-C_5$	119.4	119.7	119.4	119.4	119.5	
$\angle C_1-C_2-H_2$	119.4	119.4	119.7	119.6	119.4	
$\angle C_2-C_3-H_3$	119.5	119.7	119.7	119.7	119.7	
$\angle C_3-C_4-H_4$	120.3	120.2	120.3	120.3	120.3	
Energy (a.u.)[d]	−0.1316	−1.6918		−0.2730	−2.9320	

[a]From polarized double-ζ double zeta polarized (DZP) basis set. $E_{\mathrm{CASSCF}}=-460.505\ 48$ a.u.
[b]Reference 75.
[c]Reference 83.
[d]Energy=ground state energy+460.0.

The biphenyl molecule has 60 fundamentals which are of $11a_g$, $4a_u$, $10b_{1g}$, $6b_{1u}$, $6b_{2g}$, $10b_{2u}$, $3b_{3g}$, and $10b_{3u}$ (10) symmetries for the coplanar (D_{2h}) structure. When the molecule twists (D_2), these modes factor into $15a+16b_1+16b_2+13b_3$. Before describing the details, we note that the vibrational frequencies for the twisted structure from the HF and IVO-CASCI methods are all real, whereas for the coplanar geometry these calculations produce an *imaginary* frequency

TABLE VIII. Computed equilibrium geometry for the coplanar biphenyl molecule from 6-31G* basis set calculations. The bond angles, bond distances, and relative energy with respect to the twisted geometry are given in degrees, angstrom, and kJ/mol, respectively. The bond lengths and bond angles given here are the differences with respect to experiment.

Parameters	HF	MP2	IVO-CASCI	CASSCF[a]	DFT	Expt.[b]
ϕ	0.0	0.0	0.0	0.0	0.0	0.0
C_1-C_1'	0.002	0.010	0.001	0.001	−0.001	1.496
C_1-C_2	0.001	0.026	0.012	0.012	0.015	1.397
C_2-C_3	0.002	0.022	0.008	0.008	0.009	1.388
C_3-C_4	0.001	0.026	0.011	0.011	0.014	1.385
C_2-H_2	0.030	0.090	0.030	0.030	0.084	1.00
C_3-H_3	0.013	0.030	0.014	0.014	0.027	1.06
C_4-H_4	0.053	0.071	0.053	0.053	0.066	1.02
$\angle C_2-C_1-C_6$	−1.000	−0.800	−1.000	−1.00	−1.100	117.9
$\angle C_1-C_2-C_3$	0.700	0.600	0.700	0.700	0.008	120.9
$\angle C_2-C_3-C_4$	0.200	−0.200	0.200	0.200	−0.200	120.7
$\angle C_3-C_4-C_5$	0.000	0.000	0.000	0.100	0.000	118.9
$\angle C_1-C_2-H_2$	−1.800	−2.100	1.800	1.800	−2.100	122.4
$\angle C_2-C_3-H_3$	−1.300	−2.100	−1.200	−1.20	−1.200	120.6
$\angle C_3-C_4-H_4$	0.000	−0.100	0.100	0.100	0.000	120.6
rms deviation[c]	0.02	0.05	0.02	0.02	0.04	
ΔE_0[d]	7.5	11.4	5.2	5.2	4.0	
CPU (sec)[e]	6	72	47	160[f]	78	
Energy (a.u.)[g]	−0.0907	−1.1281	−0.2441	−0.2441	−2.8985	

[a]Same active space as employed in IVO-CASCI calculations.
[b]Reference 82.
[c]rms deviation in C–H and C–C bond lengths.
[d]$\Delta E_0=(E_{\phi=0}-E_{\mathrm{twisted}})^{\mathrm{theory}}-(E_{\phi=0}-E_{\mathrm{twisted}})^{\mathrm{expt}}$.
[e]CPU time for one energy+gradient calculations.
[f]Calculations use the GAMESS package.
[g]Energy=ground state energy+460.0.

TABLE IX. Computed equilibrium geometry for the coplanar biphenyl molecule from the pc-1 basis set (except for the CASSCF) calculation. Entries (for bond angles and bond lengths) are the differences with respect to experiment. The bond angles, bond distances, and energy are given in degrees, angstrom, and kJ/mol, respectively.

Parameters	HF	MP2	CASSCF[a,b]	IVO-CASCI	DFT	Expt.[c]
ϕ	0.0	0.0	0.0	0.0	0.0	0.0
C_1-C_1'	0.001	−0.006	0.001	−0.001	−0.003	1.497
C_1-C_2	0.002	0.012	0.012	−0.002	0.011	1.397
C_2-C_3	0.005	0.007	0.009	−0.005	0.005	1.388
C_3-C_4	0.003	0.011	0.013	−0.003	0.009	1.385
C_2-H_2	0.074	0.084	0.074	0.074	0.087	1.00
C_3-H_3	0.017	0.027	0.017	0.017	0.030	1.06
C_4-H_4	0.057	0.067	0.057	0.057	0.070	1.02
$\angle C_2-C_1-C_6$	−1.000	−0.700	−1.000	−1.000	−1.300	117.9
$\angle C_1-C_2-C_3$	0.007	0.500	0.700	0.700	0.900	120.9
$\angle C_2-C_3-C_4$	−0.200	−0.100	−0.200	−0.200	−0.200	120.7
$\angle C_3-C_4-C_5$	−0.100	0.000	−0.001	−0.100	−0.100	118.9
$\angle C_1-C_2-H_2$	−1.700	−1.900	−1.700	−1.700	−2.300	122.4
$\angle C_2-C_3-H_3$	−1.300	−1.300	−1.200	−1.300	−1.200	120.6
$\angle C_3-C_4-H_4$	0.000	0.009	0.000	0.000	0.000	120.6
rms deviation[d]	0.03	0.04	0.04	0.04	0.04	
ΔE_0[e]	7.9	12.1	4.9	6.6	4.2	
Energy (a.u.)[f]	−0.1263	−1.6849		−0.2682	−2.9281	

[a]From polarized double-ζ (DZP) basis set. $E_{\mathrm{CASSCF}}(\phi=44.3)=-460.505\ 48$ a.u.
[b]Reference 75.
[c]Reference 82.
[d]rms deviation in C–H and C–C bond lengths.
[e]$\Delta E_0=(E_{\phi=0}-E_{\mathrm{twisted}})^{\mathrm{theory}}-(E_{\phi=0}-E_{\mathrm{twisted}})^{\mathrm{expt}}$.
[f]Energy=ground state energy+460.0.

for the torsional mode (a_u symmetry). Thus, these results clearly indicate that the twisted form (D_2) is the true minimum.

Selected HF and IVO-CASCI harmonic vibrational frequencies for the twisted geometry are compared with the experiment[87] and with earlier correlated calculations[79] in Table XII. The frequencies computed with the IVO-CASCI method agree favorably with the experiment[87] and with DFT/B3LYP predictions.[79] For example, the lowest fundamental (torsional mode) 1a frequency is predicted to be 62 cm^{-1} by

TABLE X. Computed equilibrium geometry for the D_{2d} perpendicular biphenyl molecule from 6-31G* basis set calculations. The bond angles, bond distances, and ΔE (stabilization energy) energies are given in degrees, angstrom, and kJ/mol, respectively.

Parameters	HF	MP2	IVO-CASCI	DFT	Expt.[a,b]
ϕ	90.0	90.0	90.0	90.0	
C_1-C_1'	1.496	1.501	1.496	1.498	
C_1-C_2	1.392	1.416	1.403	1.407	
C_2-C_3	1.388	1.413	1.398	1.399	
C_3-C_4	1.388	1.413	1.399	1.400	
C_2-H_2	1.074	1.093	1.074	1.086	
C_3-H_3	1.074	1.092	1.073	1.086	
C_4-H_4	1.074	1.091	1.073	1.086	
$\angle C_2-C_1-C_6$	118.8	118.2	118.8	118.6	
$\angle C_1-C_2-C_3$	120.7	120.5	120.7	120.7	
$\angle C_2-C_3-C_4$	120.2	120.1	120.1	120.2	
$\angle C_3-C_4-C_5$	119.6	119.9	119.6	119.7	
$\angle C_1-C_2-H_2$	119.4	118.6	119.4	119.2	
$\angle C_2-C_3-H_3$	119.8	119.6	119.8	119.8	
$\angle C_3-C_4-H_4$	120.2	120.1	120.2	120.2	
ΔE[c]	6.9	6.6	5.2	11.6	6.5 ± 2.0
Energy (a.u.)[d]	−0.093 25	−1.1321	−0.2463	−2.8978	

[a]Reference 83.
[b]Reference 84.
[c]Energy=ground state energy+460.0.
[d]$\Delta E=E_{\mathrm{twisted}}-E_{\phi=90}$.

TABLE XI. Computed equilibrium geometry for the D_{2d} perpendicular biphenyl molecule from pc-1 basis set (except for CASSCF) calculations. The bond angles, bond distances, and energies are given in degrees, angstrom, and kJ/mol, respectively.

Parameters	HF	MP2	CASSCF[a,b]	IVO-CASCI	DFT	Expt.[c,d]
ϕ	90.0	90.0	90.0	90.0	90.0	
C_1-C_1'	1.495	1.485	1.497	1.495	1.495	
C_1-C_2	1.389	1.402	1.403	1.399	1.402	
C_2-C_3	1.385	1.397	1.400	1.394	1.396	
C_3-C_4	1.384	1.397	1.400	1.394	1.396	
C_2-H_2	1.077	1.087	1.077	1.077	1.090	
C_3-H_3	1.078	1.088	1.077	1.077	1.090	
C_4-H_4	1.077	1.087	1.077	1.077	1.090	
$\angle C_2-C_1-C_6$	118.9	119.1	118.8	118.9	118.7	
$\angle C_1-C_2-C_3$	120.6	120.2	120.7	120.6	120.7	
$\angle C_2-C_3-C_4$	120.2	120.1	120.1	120.1	120.2	
$\angle C_3-C_4-C_5$	119.6	120.0	119.6	119.7	119.6	
$\angle C_1-C_2-H_2$	119.5	119.4	119.5	119.4	119.3	
$\angle C_2-C_3-H_3$	119.7	119.8	119.8	119.8	119.8	
$\angle C_3-C_4-H_4$	120.2	120.1	120.2	120.2	120.2	
ΔE [e]	2.9	3.9	4.1	2.4	7.1	6.5 ± 2.0
Energy (a.u.)[f]	−0.1304	−1.6903		−0.2721	−2.9293	

[a]From polarized double-ζ (DZP) basis set. $E_{CASSCF}(\phi=44.3)=-460.505\ 48$ a.u.
[b]Reference 75.
[c]Reference 83.
[d]Reference 84.
[e]$\Delta E=E_{twisted}-E_{\phi=90}$.
[f]Energy=ground state energy+460.0.

the IVO-CASCI method and observed at 70 cm^{-1}; the second lowest unobserved fundamental $1b_1$ is located at 101 cm^{-1} and the corresponding DFT/B3LYP value is 92 cm^{-1}; the third fundamental $1b_2$ is observed at 116 cm^{-1} and the IVO-CASCI frequency is 131 cm^{-1}. The vibrational frequencies reported by Lee[79] are scaled by 0.963 to improve the agreement with the experiment, whereas the quoted HF and IVO-CASCI frequencies are all unscaled. The low lying vibrational frequencies (a, b_1, and b_2) are well reproduced in our scheme. Further analysis of Table XII indicates that the difference between IVO-CASCI and DFT predicted vibrational frequencies also diminishes if the IVO-CASCI frequencies are also scaled by 0.963.

3. Perpendicular geometry (D_{2d})

Tables X and XI, respectively, display the geometry of the perpendicular conformer from HF, MP2, DFT, and IVO-CASCI calculations with the 6-31G* and pc-1 basis sets. The rotational barrier height (E_{90}) determined from electron diffraction is 6.5 ± 2.0 kJ/mol. The error in the DFT calculations for E_{90} reduces substantially when the pc-1 basis is used. On the other hand, the HF, MP2, and IVO-CASCI calculations exhibit a completely opposite trend. For example, the errors in the DFT estimate of the barrier height are 5.1 and 0.6 kJ/mol for the 6-31G* and pc-1 basis sets, respectively, while the corresponding IVO-CASCI deviations are 0.08 and 4.1 kJ/mol. The difference between the barrier height computed with the HF and IVO-CASCI methods can be attributed to the differential correlation effects associated with the π-valence electrons. The data displayed in Tables X

TABLE XII. Comparison of calculated and experimental harmonic vibrational frequencies (in cm^{-1}) for the first few modes of twisted biphenyl molecule.

Symmetry	HF	IVO-CASCI	DFT[a]	Expt.[b]
a	69	62	68	70
	338	339	303	315
	474	447	407	400
	825	800	729	742
	991	908	830	838
	1114	1050	935	965
	1146	1087	982	1003
	1152	1126	1023	1030
	1333	1313	1167	1190
	1421	1407	1264	1285
	1691	1666	1499	1507
	1814	1764	1600	1612
	3351	3344	3062	3031
	3373	3365	3080	3052
	3390	3384	3092	3083
b_1	107	101	92	104
	403	389	359	360
	568	540	483	484
	697	683	605	608
b_2	135	131	125	116
	304	291	261	260
	628	588	539	545
	710	695	617	626
b_3	467	441	401	400
	693	681	601	609

[a]Reference 79.
[b]Reference 87.

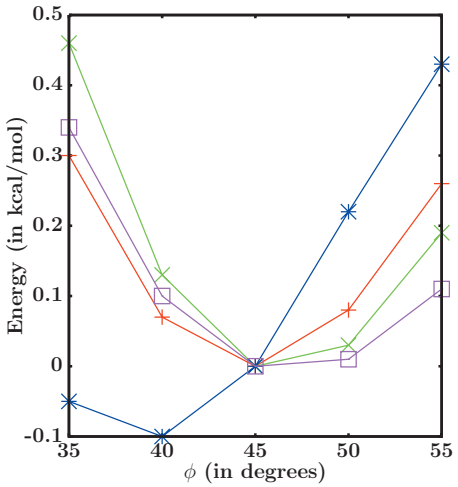

FIG. 4. The SCF (+), MP2 (×), DFT (∗), and IVO-CASCI (□) ground state energies of biphenyl molecules as a function of H_5C-CH_5 torsional angle.

and XI imply that the contribution from π-valence electron correlation to the barrier height is 0.5 (1.2) kJ/mol for 6-31G* (pc-1) basis set.

The experimental geometry for this conformer is unavailable, and hence, it is difficult to assess the accuracy of the theoretically computed quantities at this moment. However, the favorable agreement of our predicted geometries for the twisted and coplanar geometry with other theoretical and experimental data suggests that our computed spectroscopic constants for this system should be equally reliable.

We evaluate the ground state energy with all degrees of freedom frozen except for the torsional angle using the 6-31G* set. The calculations begin with the optimized geometry for the most stable conformer, i.e., the twisted geometry. The energy calculations are then repeated for torsional angles of 35°, 40°, 45°, 50°, and 55°, keeping all other degrees of freedom frozen at the twisted optimized geometry. Figure 4 presents the ground state energies of biphenyl molecule, computed as a function of the torsional angle (ϕ) using the SCF, MP2, DFT, and IVO-CASCI methods. Figure 4 clearly demonstrates that the torsional potential curve for the ground state of biphenyl is very shallow (the energy changes by less than a kcal/mol for a ±10° change in the twist/dihedral angle).

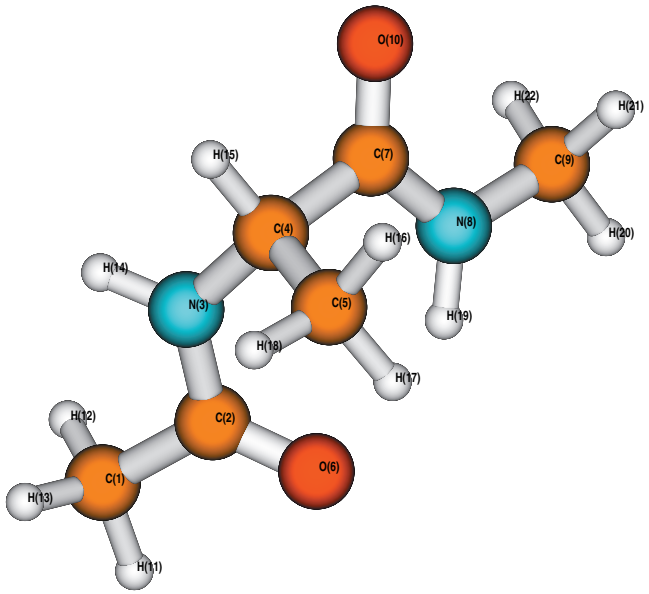

FIG. 6. Geometrical structure of alanine dipeptide (structure II).

C. Alanine dipeptide

As our last example, we consider the geometry of the alanine dipeptide ($CH_3CONHCHCH_3CONHCH_3$) molecule. Several optimized conformations of alanine dipeptide have previously been determined by Schäfer and co-workers[91,92] using the 4-21G Gaussian basis set. Force constants and vibrational frequencies of this molecule are computed by Cheam *et al.*[93] also using the 4-21G Gaussian basis set. To our knowledge, geometry optimization with the CASSCF (or MRCI) method has not been performed for this system.

The geometries depicted in Figs. 5 and 6 are optimized at with the HF, MP2, IVO-CASCI, and DFT/B3LYP approaches using the pc-1 basis set. These conformers correspond to the C_7 (Fig. 5) and C_5 (Fig. 6) structures designated by Cheam *et al.* in their *ab initio* force field studies on this system. The IVO-CASCI calculations are performed with a four-electron, six-active orbital CAS. Table XIII summarizes the elected equilibrium molecular dimensions determined from HF, MP2, IVO-CASCI, and DFT/B3LYP calculations. Also listed is the relative stability of C_7 and C_5 conformers.

As evident from Table XIII, the bond distances from the

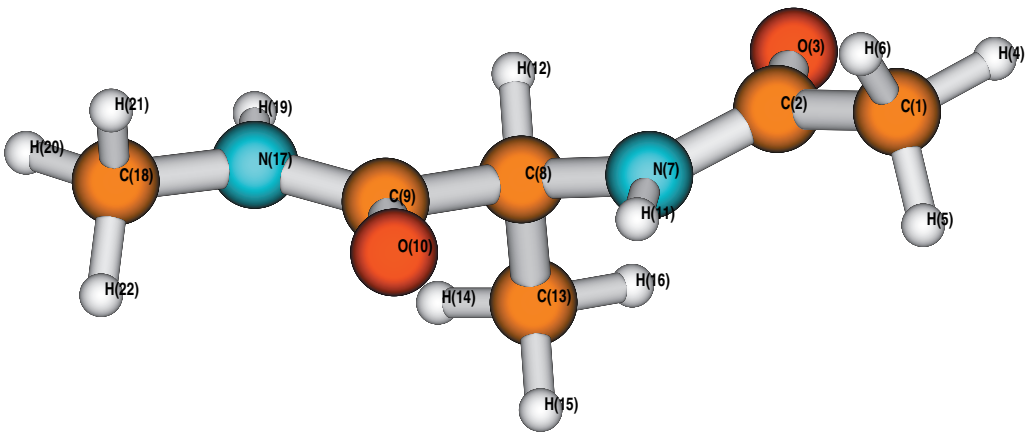

FIG. 5. Geometrical structure of alanine dipeptide (structure I).

TABLE XIII. Some representative structural parameters for the ground state of alanine dipeptide determined with various theories using the DZP basis set. Bond lengths, bond angles, and relative stability ΔE are expressed in angstrom, degrees, and Kcal/mol, respectively.

	Parameters	HF	MP2	DFT	IVO-CASCI
Structure I	r_e(C(1)–C(2))	1.506	1.510	1.518	1.507
	r_e(C(2)–O(3))	1.201	1.232	1.226	1.201
	r_e(C(2)–N(7))	1.348	1.361	1.365	1.350
	r_e(N(7)–C(8))	1.443	1.445	1.451	1.443
	r_e(C(8)–C(9))	1.522	1.524	1.535	1.523
	r_e(C(8)–C(13))	1.529	1.528	1.539	1.528
	r_e(C(9)–O(10))	1.201	1.233	1.227	1.206
	r_e(C(9)–N(17))	1.343	1.358	1.357	1.351
	r_e(N(17)–C(18))	1.448	1.451	1.455	1.447
	r_e(O(10)–H(11))	2.243	2.247	2.243	2.223
	∠(C(1)–C(2)–O(3))	122.0	122.6	122.8	122.6
	∠(C(1)–C(2)–N(7))	115.6	115.2	115.0	115.1
	∠(C(2)–N(7)–C(8))	122.5	121.5	122.5	122.6
	E_I(a.u.) [a]	−0.7429	−2.2666	− 3.4945	−0.7877
Structure II	r_e(C(1)–C(2))	1.506	1.509	1.518	1.506
	r_e(C(2)–O(6))	1.204	1.236	1.232	1.206
	r_e(C(2)–N(3))	1.347	1.359	1.362	1.360
	r_e(C(4)–C(7))	1.531	1.535	1.547	1.528
	r_e(C(4)–C(5))	1.525	1.525	1.533	1.525
	r_e(C(7)–O(10))	1.202	1.232	1.227	1.207
	r_e(C(7)–N(8))	1.339	1.354	1.353	1.349
	r_e(N(8)–C(9))	1.445	1.449	1.453	1.444
	r_e(O(6)–H(19))	2.043	1.925	1.913	2.085
	∠(C(1)–C(2)–O(6))	120.7	121.2	121.6	121.9
	∠(C(1)–C(2)–N(3))	116.1	115.6	115.4	115.1
	∠(C(2)–N(3)–C(4))	127.1	126.0	126.7	127.5
	$\Delta(E_{II}-E_I)$	9.6	3.9	4.4	1.0

[a] E_I = ground state energy + 492.0.

HF, MP2, DFT, and IVO-CASCI calculations are reasonably close to each other except for the C–O and O–H hydrogen bonds. MP2 and DFT predicted C–O bond lengths are 0.02 Å longer than those obtained from the HF and IVO-CASCI procedures, while the O–H hydrogen bond from the HF and IVO-CASCI methods is 0.1 Å longer than the MP2 and DFT estimates. Although the molecular dimensions determined from HF, MP2, IVO-CASCI, and DFT methods are reasonably close to each other, the computed relative stability (which probably arises due to hydrogen bonding and dispersion effects) varies from 1.0 to 9.6 kcal/mol. The IVO-CASCI prediction of the relative stability (1.0 kcal/mol) agrees favorably well with the earlier *ab initio* estimate of 0.95 kcal/mol.[94]

The close similarity of the geometries of the conformers from single and multireference theories indicates that alanine dipeptide has little multireference character, and, therefore, is not ideal for testing certain strengths of the IVO-CASCI method. However, the example illustrates that the method can be applied to reasonable sized systems.

IV. CONCLUSIONS

The IVO-CASCI method is extended to enable geometry optimization and the calculation of vibrational frequencies for the ground and excited states using both first and second order analytical energy gradients. Both the theoretical development and working expressions for implementing the analytic gradients within the IVO-CASCI method are presented, and the illustrations yield the following important conclusions.

(a) The present analytical gradient method is quantitatively applicable to the ground and excited states of various chemically interesting closed- and open-shell systems, and it performs satisfactorily at low computational costs.

(b) The calculated ground state geometries for the benzene, biphenyl, and alanine dipeptide molecules are generally superior to those from the HF, MP2, and DFT methods. The vibrational frequencies for benzene outperform those from the CASSCF calculations, thereby demonstrating the viability of the IVO-CASCI scheme for excited state geometry optimization.

(c) The IVO-CASCI is capable of describing ground and excited states in a reasonably balanced fashion for a given active space. The method is free of divergences and is capable of preserving symmetry during the optimization procedure. The computations are more cost effective than CASSCF treatments.

(d) The optimized geometries from the IVO-CASCI and CASSCF methods are practically identical. Thus, the existing computer codes containing the CPMCHF procedure may be used (instead of the CPMCHF proce-

dure with multiple Fock operators[43]) for frequency calculations as an approximation. While CASSCF frequency calculations with the GAMESS package are currently more time consuming than with the DALTON package, the difference can be alleviated with appropriate modification of the codes.

(e) The geometries and relative stabilities predicted by IVO-CASCI calculations for the biphenyl and alanine dipeptide molecules further demonstrate the strengths of the method.

(f) The IVO-CASCI approach is applicable to systems with broken symmetry and thus for following an intrinsic reaction path.

Thus, our IVO-CASCI analytic gradient technique can be viewed as an efficient tool to provide quantitatively accurate analyses of the ground and excited state geometries and vibrational frequencies of various chemically challenging and theoretically nontrivial systems with low computational cost.

ACKNOWLEDGMENTS

This research is supported in part by the Department of Science and Technology (DST), India (Grant No. SR/S1/PC-32/2005) and the NSF (Grant No. CHE-0749788). The authors also thank Dr. Jeff Hammond for helpful discussions.

[1] P. Pulay and W. Meyer, J. Mol. Spectrosc. **40**, 59 (1971).
[2] N. C. Handy and H. F. Schaefer, J. Chem. Phys. **81**, 5031 (1984).
[3] P. Pulay, Mol. Phys. **17**, 197 (1969).
[4] G. Fogarasi and P. Pulay, Annu. Rev. Phys. Chem. **35**, 191 (1984).
[5] J. A. Pople, R. Krishnan, H. B. Schlegel, and J. S. Binkley, Int. J. Quantum Chem. **S13**, 225 (1979).
[6] L. Adamowicz, W. D. Laidig, and R. J. Bartlett, Int. J. Quantum Chem. **26**, 245 (1984).
[7] G. Fitzgerald, R. Harrison, W. D. Laidig, and R. J. Bartlett, J. Chem. Phys. **82**, 4379 (1985).
[8] I. L. Alberts and N. C. Handy, J. Chem. Phys. **89**, 2107 (1988).
[9] J. Gauss and D. Cremer, Chem. Phys. Lett. **138**, 131 (1987).
[10] E. A. Salter, G. W. Trucks, G. Fitzgerald, and R. J. Bartlett, Chem. Phys. Lett. **141**, 61 (1987).
[11] J. Gauss and D. Cremer, Chem. Phys. Lett. **153**, 303 (1988).
[12] G. W. Trucks, E. A. Salter, and R. J. Bartlett, Chem. Phys. Lett. **153**, 490 (1988).
[13] R. J. Bartlett, in *Geometrical Derivatives of Energy Surfaces and Molecular Properties*, edited by P. Jørgensen and J. Simons (Reidel, Dordrecht, 1986).
[14] J. F. Stanton, J. Chem. Phys. **99**, 8840 (1993); J. F. Stanton and J. Gauss, *ibid.* **101**, 8938 (1994); **103**, 8931 (1995).
[15] J. Cioslowski and J. V. Ortiz, J. Chem. Phys. **96**, 8379 (1992).
[16] K. F. Freed, Annu. Rev. Phys. Chem. **22**, 313 (1971).
[17] D. Mukherjee, R. K. Moitra, and A. Mukhopadhyay, Mol. Phys. **30**, 1861 (1975); I. Lindgren and D. Mukherjee, Phys. Rep. **151**, 93 (1987); D. Mukherjee and S. Pal, Adv. Quantum Chem. **20**, 291 (1989); D. Sinha, S. K. Mukhopadhyay, R. Chaudhuri, and D. Mukherjee, Chem. Phys. Lett. **154**, 544 (1989); D. E. Bernholdt and R. J. Bartlett, Adv. Quantum Chem. **34**, 271 (1999); S. Chattopadhyay, A. Mitra, and D. Sinha, J. Chem. Phys. **125**, 244111 (2006).
[18] B. Jeziorski and H. J. Monkhorst, Phys. Rev. A **24**, 1668 (1981); B. Jeziorski and J. Paldus, J. Chem. Phys. **88**, 5673 (1988); A. Balková, S. A. Kucharski, L. Meissner, and R. J. Bartlett, Theor. Chim. Acta **80**, 335 (1991); S. A. Kucharski, A. Balkova, P. G. Szalay, and R. J. Bartlett, J. Chem. Phys. **97**, 4289 (1992).
[19] U. S. Mahapatra, B. Datta, and D. Mukherjee, J. Chem. Phys. **110**, 6171 (1999); J. Máśik and I. Hubăc, Adv. Quantum Chem. **31**, 75 (1998); I. Hubač, J. Pittner, and P. Čársky, J. Chem. Phys. **112**, 8779 (2000); L. Adamowicz, J. P. Malrieu, and V. V. Ivanov, Int. J. Mol. Sci. **3**, 522 (2002); J. Pittner, J. Chem. Phys. **118**, 10876 (2003); S. Chattopadhyay, D. Pahari, D. Mukherjee, and U. S. Mahapatra, *ibid.* **120**, 5968 (2004); S. Chattopadhyay and U. S. Mahapatra, J. Phys. Chem. A **108**, 11664 (2004); M. Hanrath, J. Chem. Phys. **123**, 084102 (2005); C. A. Nicolaides, Int. J. Quantum Chem. **102**, 250 (2005); F. A. Evangelista, A. C. Simmonett, W. D. Allen, H. F. Schaefer III, and J. Gauss, J. Chem. Phys. **128**, 124104 (2008); T. Fang, J. Shen, and S. Li, *ibid.* **129**, 234106 (2008).
[20] M. Page, P. Saxe, G. F. Adams, and B. H. Lengsfield III, J. Chem. Phys. **81**, 434 (1984); R. Shepard, in *Modern Electronic Structure Theory, Part II*, edited by D. R. Yarkony (World Scientific, Singapore, 1995), p. 345; P. Szalay, Int. J. Quantum Chem. **55**, 151 (1995).
[21] S. Pal, Phys. Rev. A **39**, 39 (1989); D. Ajitha and S. Pal, *ibid.* **56**, 2658 (1997); J. Chem. Phys. **111**, 3832 (1999).
[22] P. M. Kozlowski and E. R. Davidson, Int. J. Quantum Chem. **53**, 149 (1995); H. Nakano, K. Hirao, and M. S. Gordon, J. Chem. Phys. **108**, 5660 (1998); H. Nakano, N. Otsuka, and K. Hirao, in *Recent Advances in Computational Chemistry*, Recent Advances in Multireference Methods Vol. 4, edited by K. Hirao (World Scientific, Singapore, 1999), p. 131.
[23] J. Pittner and J. Smydke, J. Chem. Phys. **127**, 114103 (2007).
[24] F. A. Evangelista, A. C. Simmonett, H. F. Schaefer III, D. Mukherjee, and W. D. Allen, Phys. Chem. Chem. Phys. **11**, 4728 (2009).
[25] D. M. Potts, C. M. Taylor, R. K. Chaudhuri, and K. F. Freed, J. Chem. Phys. **114**, 2592 (2001).
[26] J. P. Finley and K. F. Freed, J. Chem. Phys. **102**, 1306 (1995).
[27] J. E. Stevens, R. K. Chaudhuri, and K. F. Freed, J. Chem. Phys. **105**, 8754 (1996).
[28] C. M. Taylor, R. K. Chaudhuri, and K. F. Freed, J. Chem. Phys. **122**, 044317 (2005).
[29] Y. K. Choe, Y. Nakao, and K. Hirao, J. Chem. Phys. **115**, 621 (2001).
[30] T. Hupp, B. Engels, and A. Görling, J. Chem. Phys. **119**, 11591 (2003); D. Robinson and J. J. W. McDouall, Mol. Phys. **104**, 681 (2006).
[31] H. Sun, K. F. Freed, M. Herman, and D. L. Yeager, J. Chem. Phys. **72**, 4158 (1980).
[32] R. K. Chaudhuri and K. F. Freed, J. Chem. Phys. **122**, 204111 (2005).
[33] K. Hirao, Int. J. Quantum Chem. **44**, 517 (1992); Chem. Phys. Lett. **201**, 59 (1993).
[34] H. Nakano, J. Chem. Phys. **99**, 7983 (1993).
[35] K. Andersson, P. Å. Malmqvist, B. O. Roos, A. J. Sadlej, and K. Wolinski, J. Phys. Chem. **94**, 5483 (1990); K. Andersson, P. Å. Malmqvist, and B. O. Roos, J. Chem. Phys. **96**, 1218 (1992).
[36] R. K. Chaudhuri, K. F. Freed, S. Chattopadhyay, and U. Sinha Mahapatra, J. Chem. Phys. **128**, 144304 (2008).
[37] R. K. Chaudhuri, J. R. Hammond, K. F. Freed, S. Chattopadhyay, and U. Sinha Mahapatra, J. Chem. Phys. **129**, 064101 (2008).
[38] R. K. Chaudhuri and K. F. Freed, J. Chem. Phys. **129**, 054308 (2008).
[39] S. Chattopadhyay, R. K. Chaudhuri, and U. S. Mahapatra, J. Chem. Phys. **129**, 244108 (2008).
[40] R. K. Chaudhuri and K. F. Freed, J. Chem. Phys. **126**, 114103 (2007).
[41] A. D. Becke, J. Chem. Phys. **98**, 5648 (1993); P. J. Stephens, F. J. Devlin, C. F. Chablowski, and M. J. Frisch, J. Phys. Chem. **98**, 11623 (1994); R. H. Hertwig and W. Koch, Chem. Phys. Lett. **268**, 345 (1997).
[42] D. F. Heller, K. F. Freed, and W. M. Gelbart, J. Chem. Phys. **56**, 2309 (1972); M. G. Prais, D. F. Heller, and K. F. Freed, Chem. Phys. **6**, 331 (1974).
[43] R. K. Chaudhuri, J. E. Stevens, and K. F. Freed, J. Chem. Phys. **109**, 9685 (1998).
[44] Y. Yamaguchim and Y. Osamura, *A New Dimension in Quantum Chemistry: Analytic Derivative Methods in Ab-Initio Molecular Electronic Structure Theory* (Oxford University Press, New York, 1994).
[45] J. K. L. MacDonald, Phys. Rev. **43**, 830 (1933).
[46] S. Huzinaga and C. Arnau, Phys. Rev. A **1**, 1285 (1970); J. Chem. Phys. **54**, 1948 (1971); D. McWilliams and S. Huzinaga, *ibid.* **55**, 2604 (1971).
[47] J. Gerratt and I. M. Mills, J. Chem. Phys. **49**, 1719 (1968).
[48] M. W. Schmidt, K. K. Baldridge, J. A. Boatz, S. T. Elbert, M. S. Gordon, J. H. Jensen, S. Koseki, N. Matsunaga, K. A. Nguyen, S. J. Su, T. L. Windus, M. Dupuis, and J. A. Montgomery, J. Comput. Chem. **14**, 1347 (1993).
[49] J. H. Callomon, T. M. Dunn, and I. M. Mills, Philos. Trans. R. Soc. London, Ser. A **259**, 499 (1966).
[50] B. L. Crawford and F. A. Miller, J. Chem. Phys. **17**, 249 (1949).
[51] D. H. Whiffen, Proc. R. Soc. London, Ser. A **248**, 131 (1955).
[52] S. N. Thakur, L. Goodman, and A. G. Ozkabak, J. Chem. Phys. **84**, 6642 (1986); A. G. Ozkabak and L. Goodman, *ibid.* **87**, 2564 (1987); K.

Krogh-Jespersen, R. P. Rava, and L. Goodman, J. Phys. Chem. **88**, 5503 (1984).
[53] L. Goodman, A. G. Ozkabak, and S. N. Thakur, J. Phys. Chem. **95**, 9044 (1991).
[54] B. S. Hudson and L. D. Ziegler, *The Vibronic Spectroscopy of Benzene: Old Problems and New Techniques* (Academic, New York, 1982), Vol. 5, pp. 41–140.
[55] S. Shaik, A. Shurki, D. Danovich, and P. C. Hiberty, J. Am. Chem. Soc. **118**, 666 (1996).
[56] G. H. Atkinson and C. S. Parmenter, J. Mol. Spectrosc. **73**, 20 (1978).
[57] G. Orlandi, P. Palmieri, R. Tarroni, F. Zerbetto, and M. Z. Zgierski, J. Chem. Phys. **100**, 2458 (1994).
[58] P. Swiderek, G. Hohlneicher, S. A. Maluendes, and M. Dupuis, J. Chem. Phys. **98**, 974 (1993).
[59] P. Pulay, G. Fogarasi, and J. E. Boggs, J. Chem. Phys. **74**, 3999 (1981).
[60] H. Guo and M. Karplus, J. Chem. Phys. **89**, 4235 (1988).
[61] A. G. Ozkabak, L. Goodman, and K. B. Wiberg, J. Chem. Phys. **92**, 4115 (1990).
[62] Y. Haas and S. Zilberg, J. Am. Chem. Soc. **117**, 5387 (1995).
[63] G. S. Jas and K. Kuczera, Chem. Phys. **214**, 229 (1997).
[64] D. Feller, J. Comput. Chem. **17**, 1571 (1996); K. L. Schuchardt, B. T. Didier, T. Elsethagen, L. Sun, V. Gurumoorthi, J. Chase, J. Li, and T. L. Windus, J. Chem. Inf. Model. **47**, 1045 (2007).
[65] DALTON, a molecular electronic structure program, Release 1.2 (2001), written by T. Helgaker, H. J. Aa. Jensen, P. Joergensen, J. Olsen, K. Ruud, H. Aagren, A. A. Auer, K. L. Bak, V. Bakken, O. Christiansen, S. Coriani, P. Dahle, E. K. Dalskov, T. Enevoldsen, B. Fernandez, C. Haettig, K. Hald, A. Halkier, H. Heiberg, H. Hettema, D. Jonsson, S. Kirpekar, R. Kobayashi, H. Koch, K. V. Mikkelsen, P. Norman, M. J. Packer, T. B. Pedersen, T. A. Ruden, A. Sanchez, T. Saue, S. P. A. Sauer, B. Schimmelpfennig, K. O. Sylvester-Hvid, P. R. Taylor, and O. Vahtras.
[66] B. P. Stoicheff, Can. J. Phys. **32**, 339 (1954).
[67] E. N. Lassettre, A. Skerbele, M. A. Dillon, and K. J. Ross, J. Chem. Phys. **48**, 5066 (1968).
[68] J. P. Doering, J. Chem. Phys. **51**, 2866 (1969); R. Bonneau, J. Joussot-Dubien, and R. Bensasson, Chem. Phys. Lett. **3**, 353 (1969).
[69] W. Moffitt and A. D. Liehr, Phys. Rev. **106**, 1195 (1957).
[70] W. J. Buma, J. H. van der Waals, and M. C. van Hemert, J. Am. Chem. Soc. **111**, 86 (1989).
[71] W. E. Donath, J. Chem. Phys. **42**, 118 (1965); J. H. van der Waals, A. M. D. Berghuis, and M. S. de Groot, Mol. Phys. **13**, 301 (1967); J. van Egmond and J. H. van der Waals, *ibid.* **28**, 457 (1974); S. R. Langhoff, E. R. Davidson, and C. W. Kern, J. Chem. Phys. **63**, 4800 (1975).
[72] J. Almlöf, Chem. Phys. **6**, 135 (1974).
[73] S. Tsuzuki and S. Tanabe, J. Phys. Chem. **95**, 139 (1991).
[74] G. H. Penner, J. Mol. Struct.: THEOCHEM **137**, 121 (1986).
[75] M. Rubio, M. Merchan, and E. Orti, Theor. Chim. Acta **91**, 17 (1995).
[76] G. Häfelinger and C. Regelmann, J. Comput. Chem. **6**, 368 (1985).
[77] G. Häfelinger and C. Regelmann, J. Comput. Chem. **8**, 1057 (1987).
[78] Y. Takei, T. Yamaguchi, Y. Osamura, K. Fuke, and K. Kaya, J. Phys. Chem. **92**, 577 (1988).
[79] S. Y. Lee, Bull. Korean Chem. Soc. **19**, 93 (1998) and references therein.
[80] M. Rubio, M. Merchan, E. Orti, and B. O. Roos, Chem. Phys. Lett. **234**, 373 (1995).
[81] R. J. Kurland and W. B. Wise, J. Am. Chem. Soc. **86**, 1877 (1964).
[82] L. A. Carreira and T. G. Towns, J. Mol. Struct. **41**, 1 (1977).
[83] A. Almenningen, O. Bastiansen, L. Fernholt, B. N. Cyvin, S. J. Cyvin, and S. Samdal, J. Mol. Struct. **128**, 59 (1985).
[84] O. Bastiansen and S. Samdal, J. Mol. Struct. **128**, 115 (1985).
[85] M. Akiyama, T. Watanabe, and M. Kakihana, J. Phys. Chem. **90**, 1752 (1986).
[86] H. S. Im and E. R. Bernstein, J. Chem. Phys. **88**, 7337 (1988).
[87] G. Zerbi and S. Sandroni, Spectrochim. Acta, Part A **24**, 483 (1968).
[88] Y. Sasaki and H. O. Hamaguchi, Spectrochim. Acta, Part A **50**, 1475 (1994).
[89] R. M. Barrett and D. Steele, J. Mol. Struct. **11**, 105 (1972).
[90] F. Jensen, J. Chem. Phys. **115**, 9113 (2001); **116**, 7372 (2002); **118**, 2459 (2003).
[91] L. Schäfer, C. van Alsenoy, and J. N. Scarsdale, J. Chem. Phys. **76**, 1439 (1982).
[92] J. N. Scarsdale, C. van Alsenoy, V. J. Klimkowski, L. Schäfer, and F. A. Momany, J. Am. Chem. Soc. **105**, 3438 (1983).
[93] T. C. Cheam and S. Krimm, J. Mol. Struct.: THEOCHEM **206**, 173 (1990).
[94] G. A. Kaminski, R. A. Friesner, J. Tirado-Rives, and W. L. Jorgensen, J. Phys. Chem. B **105**, 6474 (2001).